

AD-A063 147

HONEYWELL INC MINNEAPOLIS MN AVIONICS DIV
ADVANCED FLUIDIC TEMPERATURE STUDIES.(U)
OCT 78 W M POSINGIES
W0454FR1

F/G 13/7

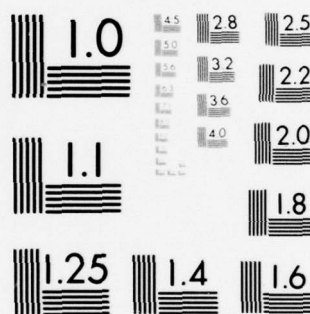
UNCLASSIFIED

DAAJ02-77-C-0036
NL

USARTL-TR-78-33

1 OF 1
AD
A063147





MICROCOPY RESOLUTION TEST CHART
NATIONAL BUREAU OF STANDARDS-1963-A

AD A063147

USARTL-TR-78-33

LEVEL

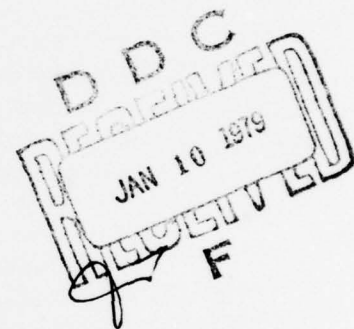
(12)

2



ADVANCED FLUIDIC TEMPERATURE STUDIES

Walter M. Posingies
HONEYWELL INC.
Avionics Division
Minneapolis, Minn. 55413



October 1978

Final Report for Period 1 August 1977 - 31 March 1978

Approved for public release;
distribution unlimited.

Prepared for
APPLIED TECHNOLOGY LABORATORY
U. S. ARMY RESEARCH AND TECHNOLOGY LABORATORIES (AVRADCOM)
Fort Eustis, Va. 23604

79 01 08 032

DDC FILE COPY.

APPLIED TECHNOLOGY LABORATORY POSITION STATEMENT

This report has been reviewed by the Applied Technology Laboratory, U. S. Army Research and Technology Laboratories (AVRADCOM) and is considered to be technically sound.

This research effort resulted from the need which exists to overcome the sensitivity which hydrofluidic systems have to fluid viscosity. Since viscosity has a direct relationship to fluid temperature, this need translated into extending the fluid operating temperature range of hydrofluidic systems without substantially increasing fluid flow requirements and maintaining system gain and null variations within a $\pm 20\%$ range.

Mr. George W. Fosdick of the Applied Aeronautics Technical Area, Aeronautical Systems Division, served as project engineer for this effort.

DISCLAIMERS

The findings in this report are not to be construed as an official Department of the Army position unless so designated by other authorized documents.

When Government drawings, specifications, or other data are used for any purpose other than in connection with a definitely related Government procurement operation, the United States Government thereby incurs no responsibility nor any obligation whatsoever; and the fact that the Government may have formulated, furnished, or in any way supplied the said drawings, specifications, or other data is not to be regarded by implication or otherwise as in any manner licensing the holder or any other person or corporation, or conveying any rights or permission, to manufacture, use, or sell any patented invention that may in any way be related thereto.

Trade names cited in this report do not constitute an official endorsement or approval of the use of such commercial hardware or software.

DISPOSITION INSTRUCTIONS

Destroy this report when no longer needed. Do not return it to the originator.

Unclassified

SECURITY CLASSIFICATION OF THIS PAGE (When Data Entered)

REPORT DOCUMENTATION PAGE		READ INSTRUCTIONS BEFORE COMPLETING FORM
1. REPORT NUMBER USARTL-TR-78-33	2. GOVT ACCESSION NO.	3. RECIPIENT'S CATALOG NUMBER
4. TITLE (and Subtitle) ADVANCED FLUIDIC TEMPERATURE STUDIES		5. TYPE OF REPORT & PERIOD COVERED FINAL REPORT 1 Aug., 1977-31 March 1978
6. AUTHOR(s) Walter M. Posingies		7. PERFORMING ORG. REPORT NUMBER WC454FR1
8. PERFORMING ORGANIZATION NAME AND ADDRESS Honeywell Inc. Avionics Division Minneapolis, Minnesota 55413		9. CONTRACT OR GRANT NUMBER(s) DAAJO2-77-C-0036
10. CONTROLLING OFFICE NAME AND ADDRESS Applied Technology Laboratory, U.S. Army Research and Technology Laboratories (AVRADCOM) Fort Eustis, Virginia 23604		11. PROGRAM ELEMENT, PROJECT, TASK AREA & WORK UNIT NUMBERS 63211A 1L263211D157 12 002 EK
12. MONITORING AGENCY NAME & ADDRESS (if different from Controlling Office) 79 P		13. REPORT DATE October 1978
14. DISTRIBUTION STATEMENT (of this Report) Approved for public release; distribution unlimited		15. SECURITY CLASS. (of this report) Unclassified
16. DISTRIBUTION STATEMENT (of the abstract entered in Block 20, if different from Report) Final rept. 1 Aug 77-31 Mar 78		15a. DECLASSIFICATION/DOWNGRADING SCHEDULE
18. SUPPLEMENTARY NOTES		
19. KEY WORDS (Continue on reverse side if necessary and identify by block number) Hydrofluidics Vortex Rate Sensor Viscosity Compensation Hydraulics Stability Augmentation System Fluidics		
20. ABSTRACT (Continue on reverse side if necessary and identify by block number) A Hydrofluidic Stability Augmentation System (HYSAS) developed in a previous program was modified to extend its operating temperature range. Base-line performance data, parametric test data, and a detailed analysis of the selected compensation approaches are presented. The compensated system was tested with MIL-H-5606 oil, and its gain remained within a ± 20 -percent band over the temperature range from 50° to 180°F.		

DD FORM 1 JAN 73 1473 EDITION OF 1 NOV 65 IS OBSOLETE

Unclassified

SECURITY CLASSIFICATION OF THIS PAGE (When Data Entered)

393 207

PREFACE

This document is the final report under Army Contract DAAJ02-77-C-0036. The program was administered under the direction of the Applied Technology Laboratory U.S. Army Research & Technology Laboratories (AVRADCOM), Fort Eustis, Virginia, with Mr. G. W. Fosdick as the project engineer. The work was conducted during the period 1 August 1977 through 31 March 1978.

ACQUISITION for	
NIS	State Section <input checked="" type="checkbox"/>
DDP	Self Section <input type="checkbox"/>
DISTRIBUTION	
DISTRIBUTION/AVAILABILITY CODES	
SPECIAL	
A	

TABLE OF CONTENTS

Section	Page
PREFACE.....	3
LIST OF ILLUSTRATIONS	6
LIST OF TABLES	8
I INTRODUCTION	9
II HARDWARE CONFIGURATIONS.....	11
General.....	11
YG1143 Yaw Axis Controller Original Configuration.....	11
YG1143 Controller Baseline Configuration	13
YG1143 Controller with Independent Development (I.D.) Amplifiers.....	18
YG1143 Controller with Temperature Compensation.....	18
III BASELINE AND PARAMETRIC DATA ON THE YG1143 SYSTEM WITH STANDARD AMPLIFIERS	23
IV BASELINE AND PARAMETRIC TEST DATA ON THE YG1143 HYSAS SENSOR CONTROLLER USING HONEYWELL INDEPENDENT DEVELOPMENT (I.D.) AMPLIFIERS	34
V TEMPERATURE COMPENSATION ANALYSIS.....	44
VI DEVELOPMENT TESTING.....	57
VII TESTING OF THE FINAL CONFIGURATION.....	70
VIII CONCLUSIONS.....	79

PRECEDING PAGE BLANK-NOT FILMED

LIST OF ILLUSTRATIONS

Figure		Page
1	Schematic of Original YG1143 Controller	12
2	YG1143 — Yaw Axis Controller Exploded View.....	14
3	Yaw Axis Controller Servoactuator Assembly — Side View	15
4	Yaw Axis Controller Servoactuator Assembly — Top View	15
5	Modified YG1143 Sensor Controller Schematic.....	16
6	Modified YG1143 Controller Supply and Return Connections	17
7	Modified YG1143 Controller Showing Instrumentation Connections....	19
8	Photographs of Lower Manifold Configurations	20
9	Photographs of Upper Manifold Configurations	21
10	Temperature Compensation Hardware Modifications	22
11	YG1143 System Standard Amplifiers Baseline Test — Rate Sensor and System Gain	24
12	YG1143 Component Gains as a Function of Fluid Temperature — Standard Amplifiers.....	25
13	YG1143 System with Standard Amplifiers Baseline Test — Component and System Null Offset Characteristics	26
14	YG1143 System with Standard Amplifiers Baseline Test — Flow Split versus Temperature.....	27
15	Baseline System with Standard Amplifiers Baseline Test — 120°F Frequency Response.....	29
16	YG1143 System with Standard Amplifiers — Low Temperature Parametric Investigation (40°F)	30
17	System Gains as a Function of Control Pressure Level — Standard Amplifiers, 120°F, $Q_A = 0.575 \text{ in.}^3/\text{sec}$	31
18	System Gains as a Function of Control Pressure Level — Standard Amplifiers, 180°F, $Q_A = 0.578 \text{ in.}^3/\text{sec}$	33
19	YG1143 System with I.D. Amplifiers Baseline Test — 120°F Frequency Response.....	35
20	YG1143 System with I.D. Amplifiers Baseline Test — Rate Sensor and System Gain (40° to 180°F).....	36
21	YG1143 System with I.D. Amplifiers Baseline Test — Component Gain Characteristics (40° to 180°F)	37

LIST OF ILLUSTRATIONS (Continued)

Figure		Page
22	YG1143 System with I.D. Amplifiers Baseline Test — Null Offset Characteristics (40° to 180°F)	38
23	YG1143 System with I.D. Amplifiers — Flow Split versus Temperature	39
24	YG1143 System with I.D. Amplifiers — Low Temperature Parametric Investigations (40°F).....	41
25	System Gains as a Function of Control Pressure Level — I.D. Amplifiers, 40°F, $Q_A = 1.02 \text{ in.}^3/\text{sec}$	42
26	System Gains as a Function of Control Pressure Level — I.D. Amplifiers, 120°F, $Q_A = 0.753 \text{ in.}^3/\text{sec}$	43
27	Resistances in Hydraulic Flow Paths	45
28	Flow Path Calculated Characteristic Impedances	52
29	Temperature Compensation Element — Photograph and Schematic	53
30	Coupling Element Modification.....	56
31	Configuration One System Gain Characteristics	58
32	Configuration One Component Gain Characteristics.....	59
33	Configuration One Null Offset Characteristics	60
34	Configuration One Flow Split Characteristics	61
35	Effects of Control Pressure Level on System Gain	63
36	Configuration Two System Gain Characteristics.....	64
37	Configuration Three System Gain Characteristics	65
38	Configuration Four System Gain Characteristics	66
39	Configuration Four Component Gain Characteristics	67
40	Configuration Four Null Characteristics	68

LIST OF ILLUSTRATIONS

Figure		Page
41	Configuration Four Flow Split Characteristics	69
42	Preamplifier Null Offset Study Summary	71
43	Preamplifier Bias of the Final Configuration	75
44	System Gain as a Function of Temperature — Final Configuration	76
45	System Gain as a Function of Total System Flow — Final Configuration	77

LIST OF TABLES

Table		Page
1	Coupling Element Pressure Drop as a Function of Oil Temperature or Viscosity	48
2	Rate Sensor Pickoff Pressure Drop Characteristics	49
3	Calculated Pickoff and Secondary Sink Flow Split Characteristics without Compensation	50
4	Amplifier Cascade Pressure Drop Characteristics	50
5	Calculated Pickoff and Secondary Sink Flow Split Characteristics with Compensation	54
6	YG1143 Flow Sensitivity Test Data	72
7	Power Supply Tests at 180°F	73

SECTION I INTRODUCTION

In a series of Government-sponsored programs, hydrofluidic stability augmentation systems (HYSAS) have demonstrated exceptional reliability, adequate performance, and a production cost somewhat lower than that of equivalent electronic systems. The HYSAS's capability to enhance the flying qualities of helicopters is reported in Reference 1. As reported in Reference 2, a reliability in excess of 4000 hours mean time between failures (MTBF) was demonstrated, and a 43,000-hour MTBF was projected as the result of a 16,000-hour flight test program. Development of a high yield production line for hydrofluidic systems using electroformed components is reported in Reference 3.

Hydrofluidic systems are sensitive to changes in fluid viscosity. This problem was overcome during the development of a three-axis SAS that was used on the Sikorsky UTTAS prototype helicopters. The solution, which made the hydraulic power conditioning system more complex, was to schedule flow to the hydrofluidic controllers as a function of fluid viscosity. When the hydraulic fluid temperature was cold, this system required 2.5 times as much flow as it needed at normal operating temperatures.

The objective of this program was to extend the operating temperature range of HYSAS through the use of various temperature compensation techniques within the HYSAS fluidic network without substantially increasing system flow requirements. The specific goal was to extend the operation of the existing OH-58 yaw axis HYSAS (YG1143 controller described in Reference 2) to maintain null and gain within ± 20 percent over a temperature range of 40° to 180°F when operating with MIL-H-5606 hydraulic oil at a maximum flow of 0.7 gallons per minute (gpm).

-
1. Harvey Ogren, Donald Sotanski, and LeRoy Genaw, Yaw Axis Stability Augmentation System Flight Test Report, Honeywell, USAAMRDL-TR-74-39, Eustis Directorate, U.S. Army Air Mobility R&D Laboratory, Fort Eustis, Virginia, June 1974, AD 784134.
 2. Lloyd J. Banaszak and Walter M. Posingies, HYSAS Operational Suitability Demonstration, Phase II, Honeywell Inc., USAAMRDL-TR-77-31, Applied Technology Laboratory, U.S. Army Research & Technology Laboratories (AVRADCOM), Fort Eustis, Virginia, October 1977, AD A038562.
 3. Walter Posingies, Production Suitability of an Electroform Conductive-Wax Process for the Manufacture of Fluidic Systems, Honeywell, USAAMRDL-TR-77-2, Eustis Directorate, U.S. Army Air Mobility R&D Laboratory, Fort Eustis, Virginia, April 1977, AD A047643.

This report describes the steps taken to develop a straightforward process for extending the operating temperature range of the OH-58 yaw axis HYSAS. Steps in this iterative development included obtaining parametric data, analysis, and hardware modification and testing of the modified system over the required operating temperature range. Discussions of problems encountered along with supporting test data define the type of component characteristics required for simple and practical temperature compensation. Conclusions relative to suitability of the investigated compensation techniques for future HYSAS applications are presented.

SECTION II

HARDWARE CONFIGURATIONS

GENERAL

Temperature compensation techniques were developed using one of the OH-58 yaw HYSAS sensor/controllers produced under a previous contract. This YG1143 sensor/controller was modified extensively three times during the course of this program.

Initial modifications were incorporated to permit the monitoring of internal flows and pressures. These modifications made it possible to measure baseline performance of major components in the system, including changes in flow split between major components as a function of temperature. Circuit adjustments to simplify the system were also accomplished at this time.

A second modification was required to install independent development (I.D.) amplifiers, as these amplifiers are not directly interchangeable with the original YG1143 amplifiers.

Incorporation of temperature compensation into the YG1143 system was the third modification.

YG1143 YAW AXIS CONTROLLER ORIGINAL CONFIGURATION

Figure 1 is a schematic of the original YG1143 yaw axis controller. Helicopter yaw rate is measured by a vortex rate sensor (VRS), amplified by amplifiers A₁ and A₂, high passed using series bellows capacitors, and amplified again by a double amplifier, A₄. A small portion of the rate signal bypasses the high-pass capacitors through resistors R₂₂ and R₂₃. The transfer function of this rate signal is

$$\frac{\Delta P_{\text{out}}}{\text{rate in}} = \left[0.135 \left(\frac{2.5S}{2.5S+1} \right) + 0.027 \right] e^{-0.06S} \text{ psid/deg/sec.} \quad (1)$$

A second input into this controller, the pilot input device (PID), allows the controller to damp out external disturbances without counteracting pilot inputs. A cable from the rudder pedal linkage moves the PID flow divider, whose output is lagged by capacitor C₅ and amplified by amplifier A₃. With ideal gains and shaping, the signal at the output of A₃ for a specific pilot command will

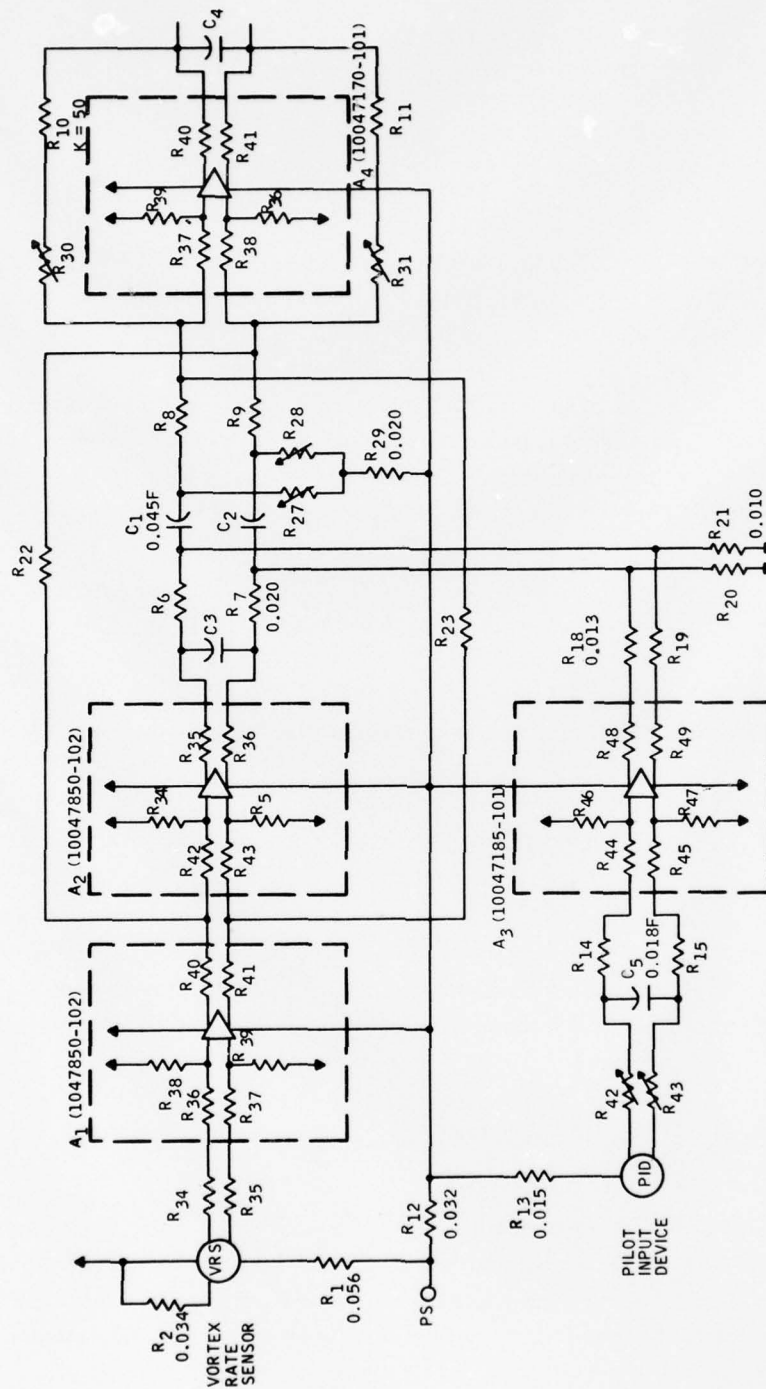


Figure 1. Schematic of Original YG1143 Controller.

be equal to and opposite in polarity from the resulting rate signal at the output of amplifier A₂. For a pilot command, the net effect change at amplifier A₄ should be nearly zero. Transfer function of this pilot loop is

$$\frac{\Delta P \text{ out}}{\text{cable travel input}} = 45.2 \left(\frac{1}{S+1} \right) \left(\frac{2.5S}{2.5S+1} \right) \frac{\text{psid}}{\text{in. of cable}} \quad (2)$$

Figure 2 is an exploded view of the YG1143 yaw axis controller. The controller housing is about 5.8 inches long by 3.3 inches wide. Brackets, fittings, and bolts are not shown in the exploded view. Figures 3 and 4 are two views of a completely assembled YG1143 controller mounted on its servo-actuator.

YG1143 CONTROLLER BASELINE CONFIGURATION

Returns from the rate sensor primary sink, the rate sensor secondary sink, the upper manifold, and the lower manifold were all connected internally in the original configuration. Figure 5 is a schematic showing how these return flow ports were modified to permit the measurement of flow in each major component. Newly installed valves, V₁ through V₅, make it possible to change the flow split between components and to change pressure level as part of a parametric analysis. Valves V₁ through V₄ were part of the external test setup; however, V₅ was built into the controller housing.

The YG1143 circuit was also simplified at this time to eliminate potential interactions that could complicate the interpretation of parametric data. Adjustments included blocking resistors R₂₂ and R₂₃ (see Figure 1) to eliminate the through rate signal as well as blocking resistors R₁₈ and R₁₉ to disable the PID. These two eliminated circuits are unique to the YG1143, and the modified circuit tested is typical of the circuits used on other applications such as the OH-58 roll axis and YUH-60 HYSAS systems. The transfer function of the baseline configurations and all subsequent configurations was approximately

$$\frac{\Delta P \text{ out}}{\text{rate in}} = 0.15 \left(\frac{2.5S}{2.5S+1} \right) e^{-0.06S} \text{ psid/deg/sec} \quad (3)$$

Figure 6 is a photograph of the modified YG1143 controller showing the mounting surface. Three new ports were added to the surface to provide a primary sink return, a secondary sink return, and a pressure tap for measuring rate sensor supply pressure. A new lower manifold adapter plate is

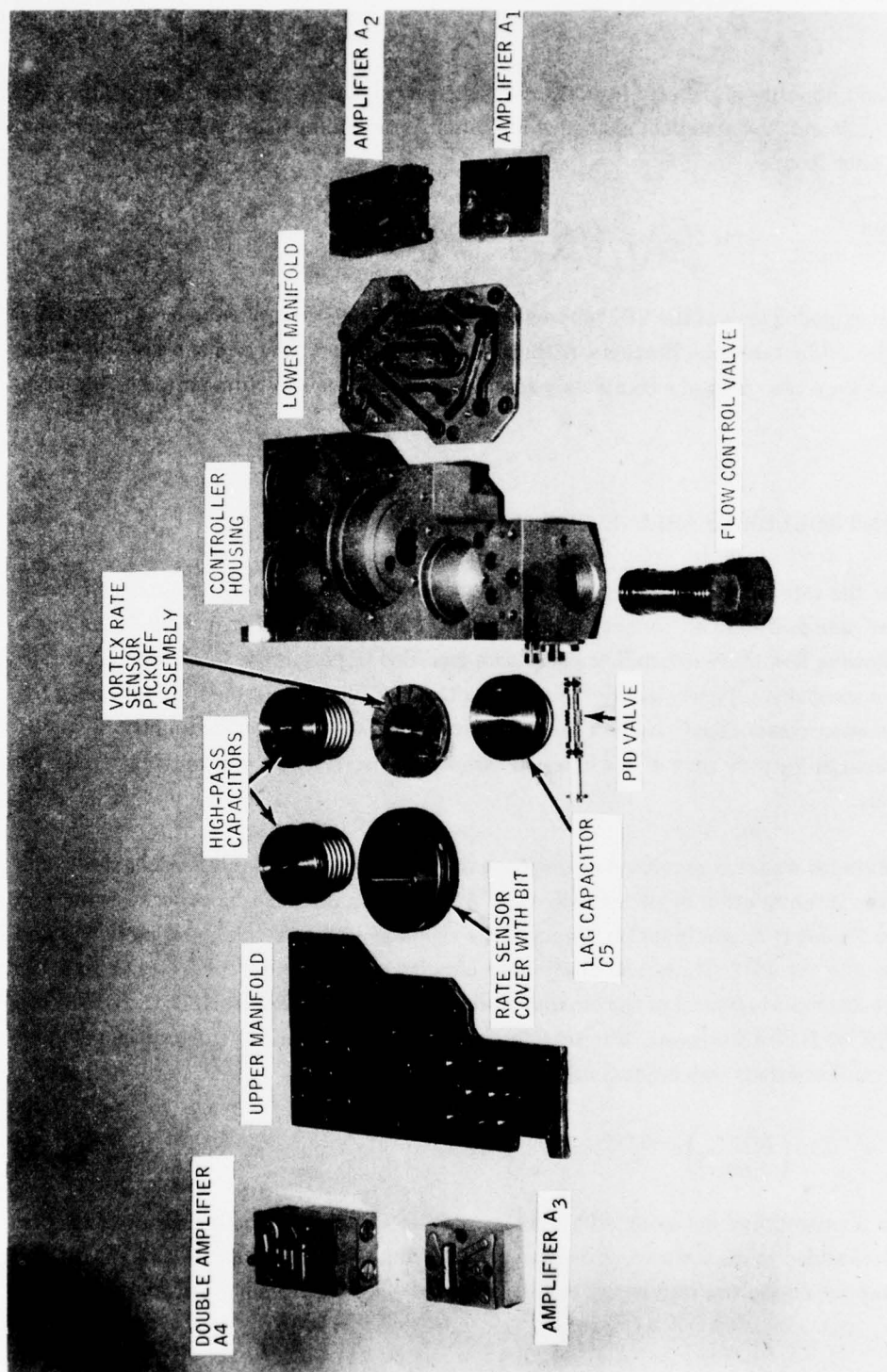


Figure 2. YG1143—Yaw Axis Controller Exploded View

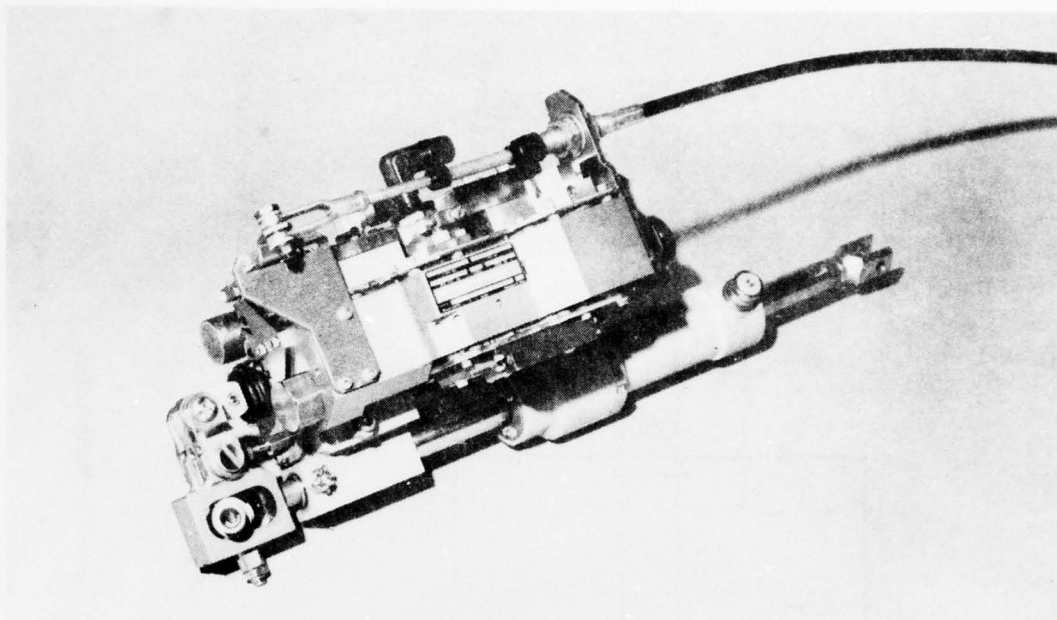


Figure 3. Yaw Axis Controller Servoactuator Assembly—Side View

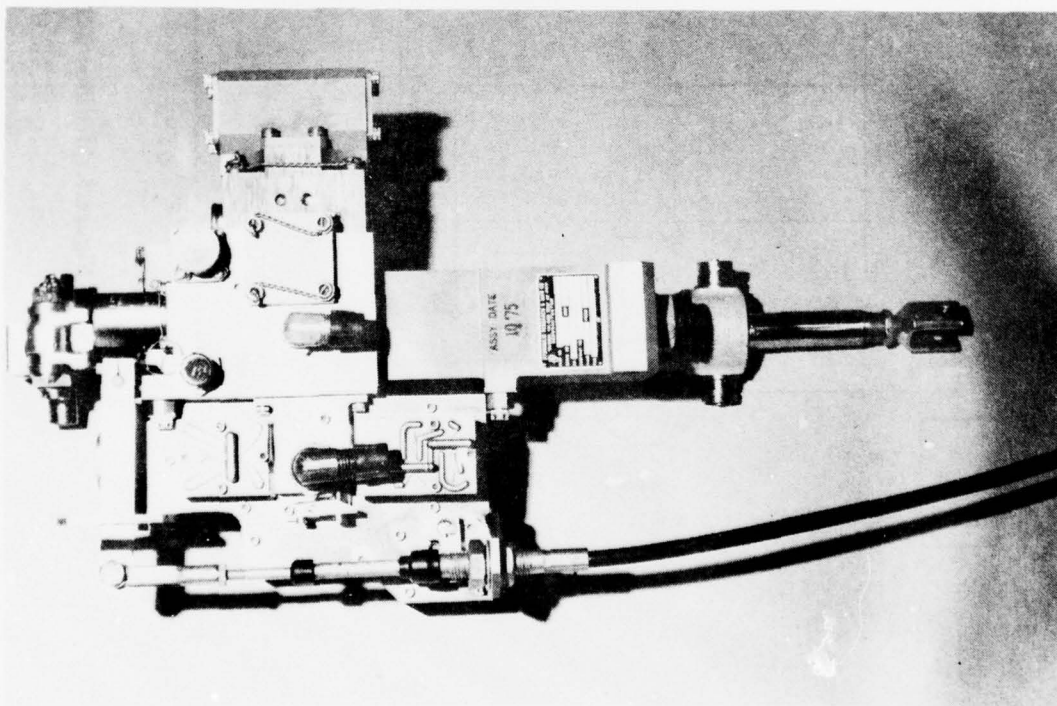


Figure 4. Yaw Axis Controller Servoactuator Assembly—Top View

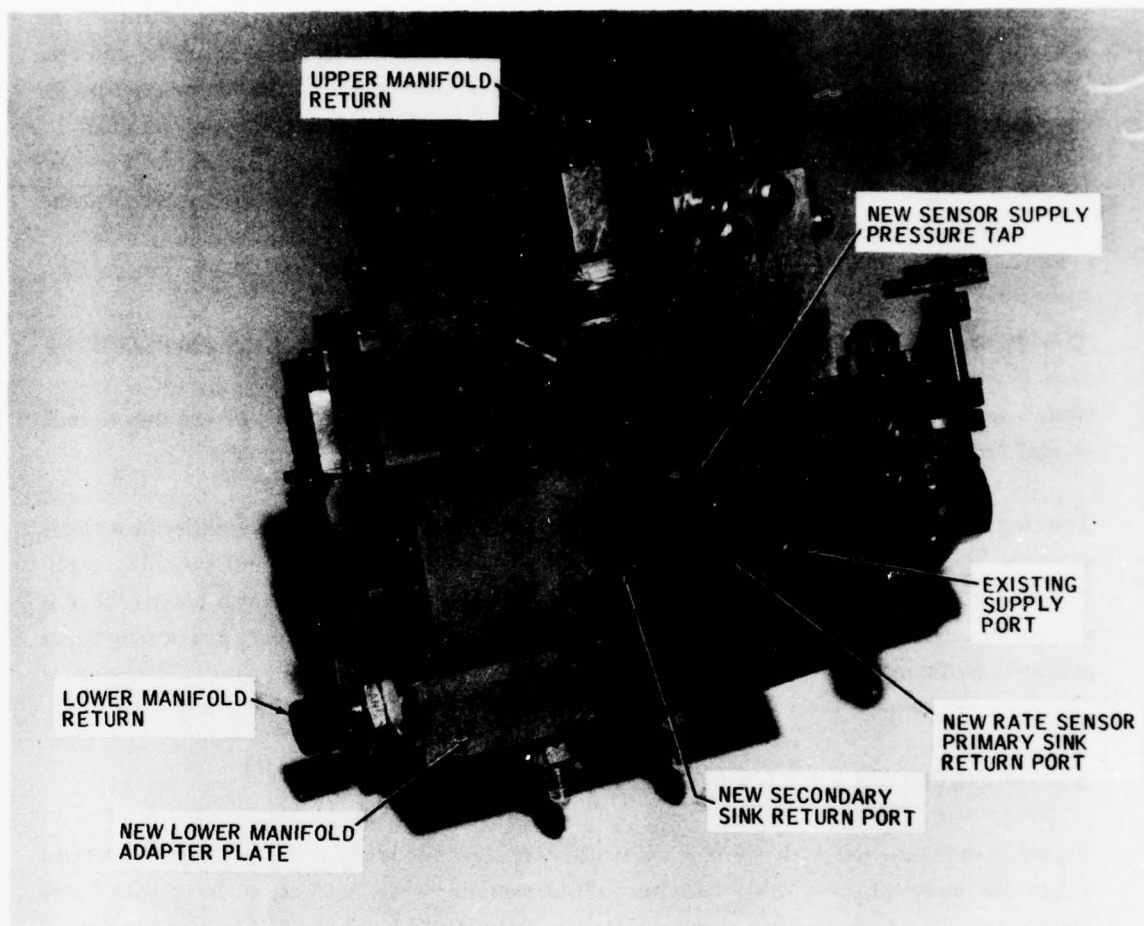


Figure 6. Modified YG1143 Controller Supply and Return Connections

visible on the bottom of the controller. This plate provides a separate hydraulic return for the preamplifier and pressure taps to allow instrumentation for measurement of amplifier and rate sensor performance. The upper manifold return at the top was originally the common return for the entire controller before an appropriate blocker was installed under the upper manifold.

Figure 7, another view of the modified controller, identifies the newly installed valve, V₅, and the adapter blocks used for the measurement of internal signals.

YG1143 CONTROLLER WITH INDEPENDENT DEVELOPMENT (I.D.) AMPLIFIERS

Manifolds were designed and fabricated to adapt the I.D. amplifiers, which replaced the original, shorter amplifiers. Figure 8 shows the lower manifold configurations.

The output amplifier cascade for the baseline configuration was a double amplifier in a single compact block. A relatively elaborate adapter block was necessary to mount two I.D. amplifiers in this same space. A reversing manifold was used at the top to obtain a polarity that is compatible with the negative feedback used around this output cascade. Figure 9 shows the upper manifold configurations.

YG1143 CONTROLLER WITH TEMPERATURE COMPENSATION

Figure 10 shows the relatively simple modifications that resulted in substantial temperature compensation improvements. Most of the rate sensor coupling elements were replaced with blank spacers to increase the coupling element viscosity sensitivity. This increased the pressure drop at cold temperature, resulting in a higher amplifier flow on this constant flow system. Resistor R₁ in the rate sensor housing was drilled out to reduce the sharp-edged orifice pressure drop across the rate sensor. A viscosity sensitive resistor was installed externally to replace R₂ in the secondary sink. This results in a greatly reduced secondary sink flow at cold temperatures, thereby allowing an increase in both primary sink flow and amplifier flow under these conditions.

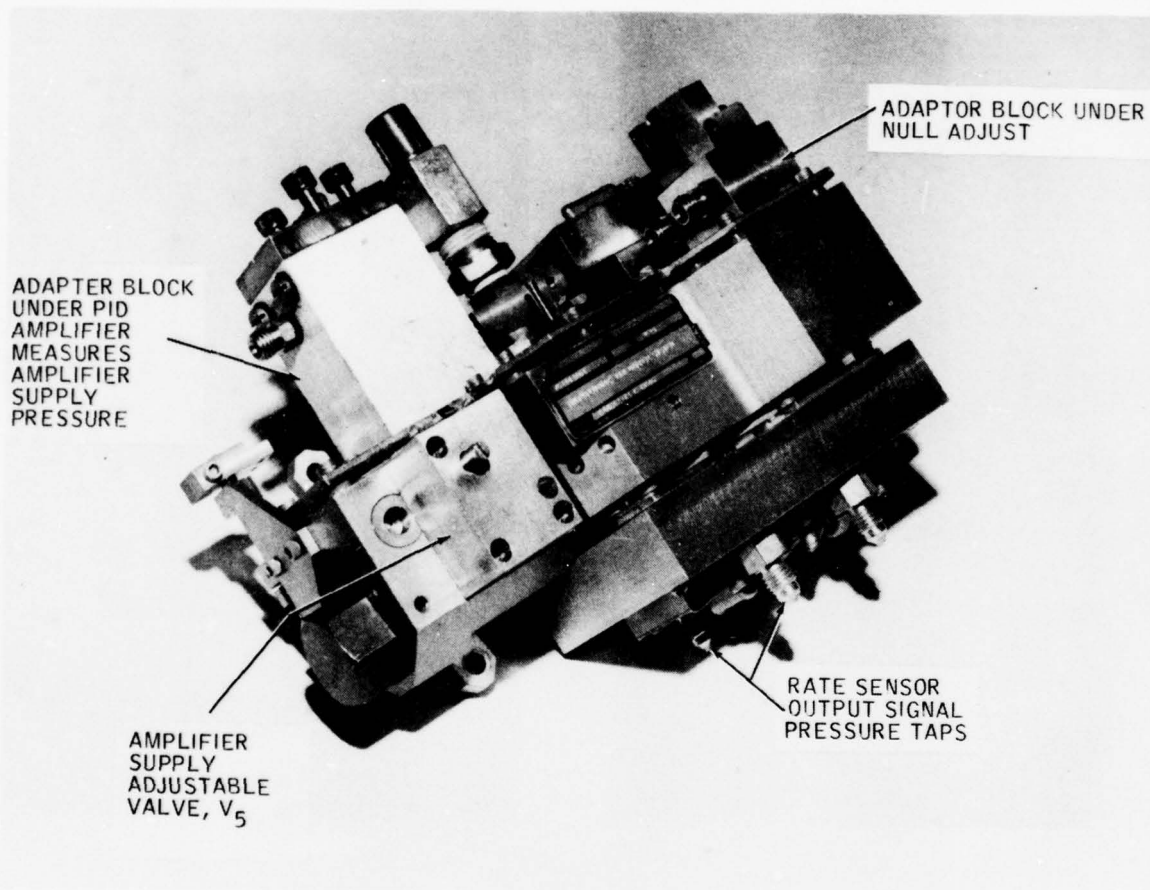


Figure 7. Modified YG1143 Controller Showing Instrumentation Connections

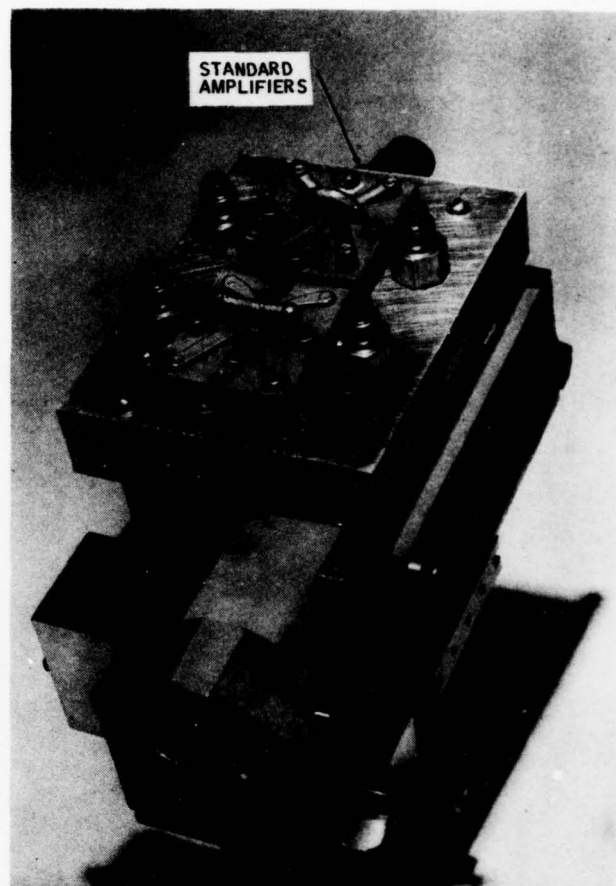
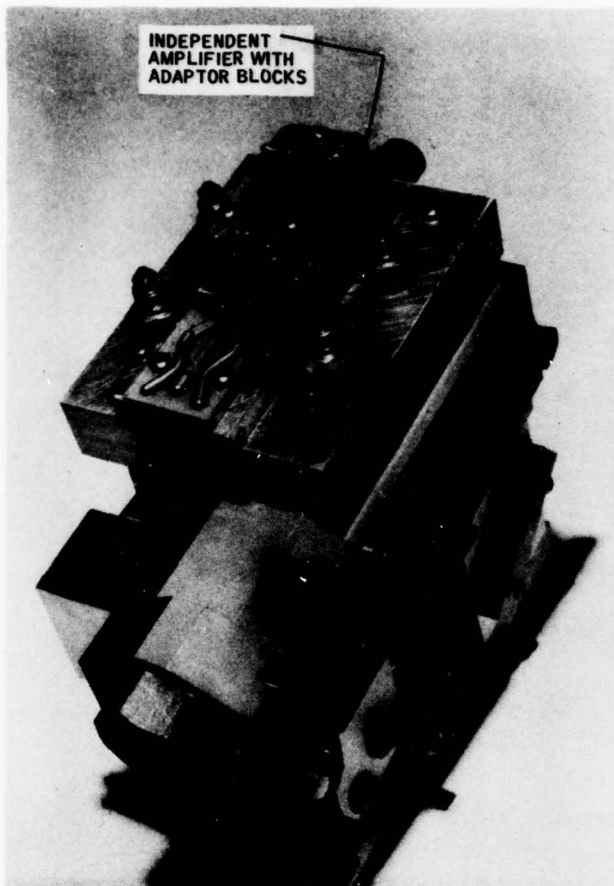


Figure 8. Photographs of Lower Manifold Configurations

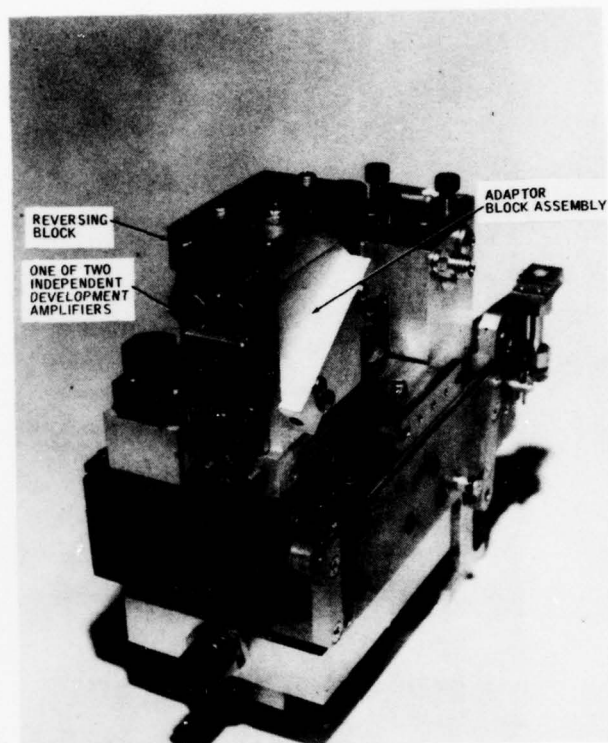
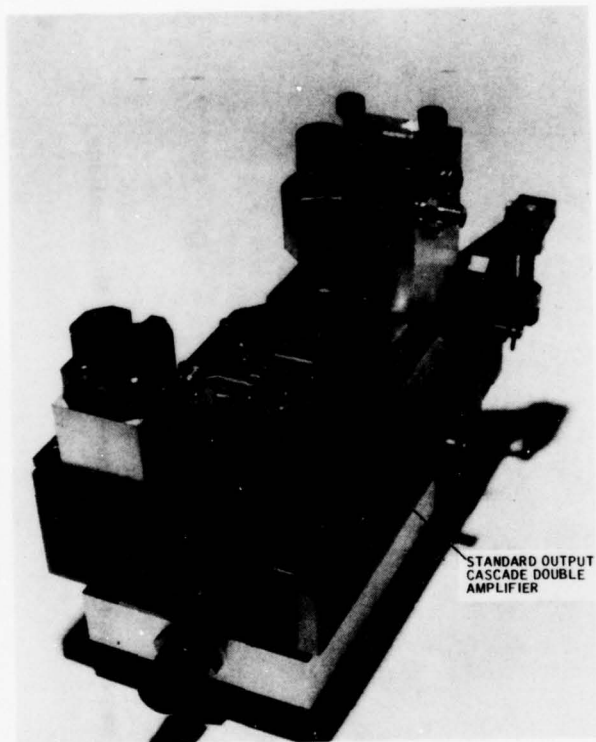


Figure 9. Photographs of Upper Manifold Configurations

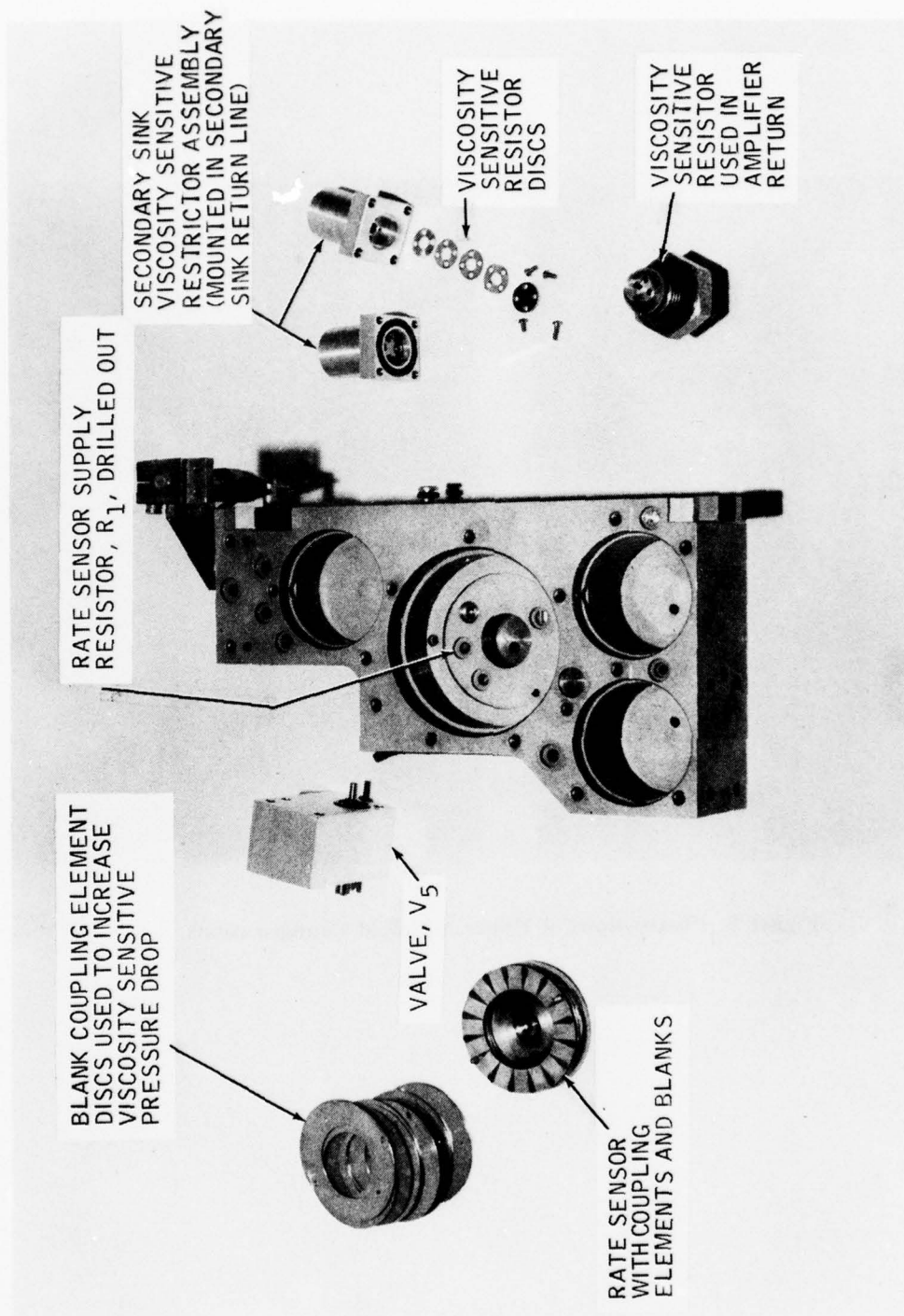


Figure 10. Temperature Compensation Hardware Modifications

SECTION III

BASLINE AND PARAMETRIC DATA ON THE YG-1143 SYSTEM WITH STANDARD AMPLIFIERS

Baseline system performance with the standard amplifiers installed on the YG1143 controller was obtained over the temperature range 40° to 180°F. Figure 11 shows system gain as a function of hydraulic fluid temperature. Performance is within the ± 20 -percent band over the temperature range from about 95° to 170°F. All gain data were plotted on a logarithmic scale so that a ± 20 -percent band is the same width at any location on the curve. Rate sensor gain plotted on this same figure is relatively constant, indicating that one or more other components are responsible for the large gain decrease at cold temperature.

Figure 12 shows the gains of the preamplifier, capacitor, and output amplifier. Most of the gain change occurs in the preamplifier. Negative feedback may have helped maintain a constant output amplifier gain above 70°F; however, this gain also decreased sharply below 70°F. Gain across the high-pass capacitor is more constant, and it increases slightly with colder temperature.

Figure 13 shows null offset as a function of temperature. Overall system output null offset remained well within the ± 0.4 -psid limit. The preamplifier null offset of 1.4 psid is relatively large for an amplifier whose range is only about ± 2 psid at high temperature. Good null offset performance at cold temperature can be largely attributed to the very low gains at cold temperature. Rate sensor null offset is plotted on a scale that is expanded by a factor of 20 over that of the preamplifier null offset. Although the rate sensor and preamplifier null offset curves appear similar in shape, the magnitude of the rate sensor shift is much too small to cause the observed preamplifier null offset. Note that the change in rate sensor null offset from 100° to 160°F was 0.032 psid, which at a nominal preamplifier gain of 10 would result in a preamplifier null offset change of only 0.32 psid. Actual preamplifier null offset change over this temperature range was 1.85 psid, which is nearly six times as large as that expected from the rate sensor null offset change.

Figure 14 shows the flow split between the primary sink, secondary sink, and amplifiers. An increase in rate sensor primary sink flow results in an increase in rate sensor gain, whereas an increase in secondary sink flow has very little effect on rate sensor gain. At cold temperature, an increase in amplifier flow would result in a large improvement in amplifier cascade gain. In Figure 14, the change in flow split between these components is opposite of that desired. Primary sink flow and amplifier flow decrease at cold temperature, and secondary sink flow increases.

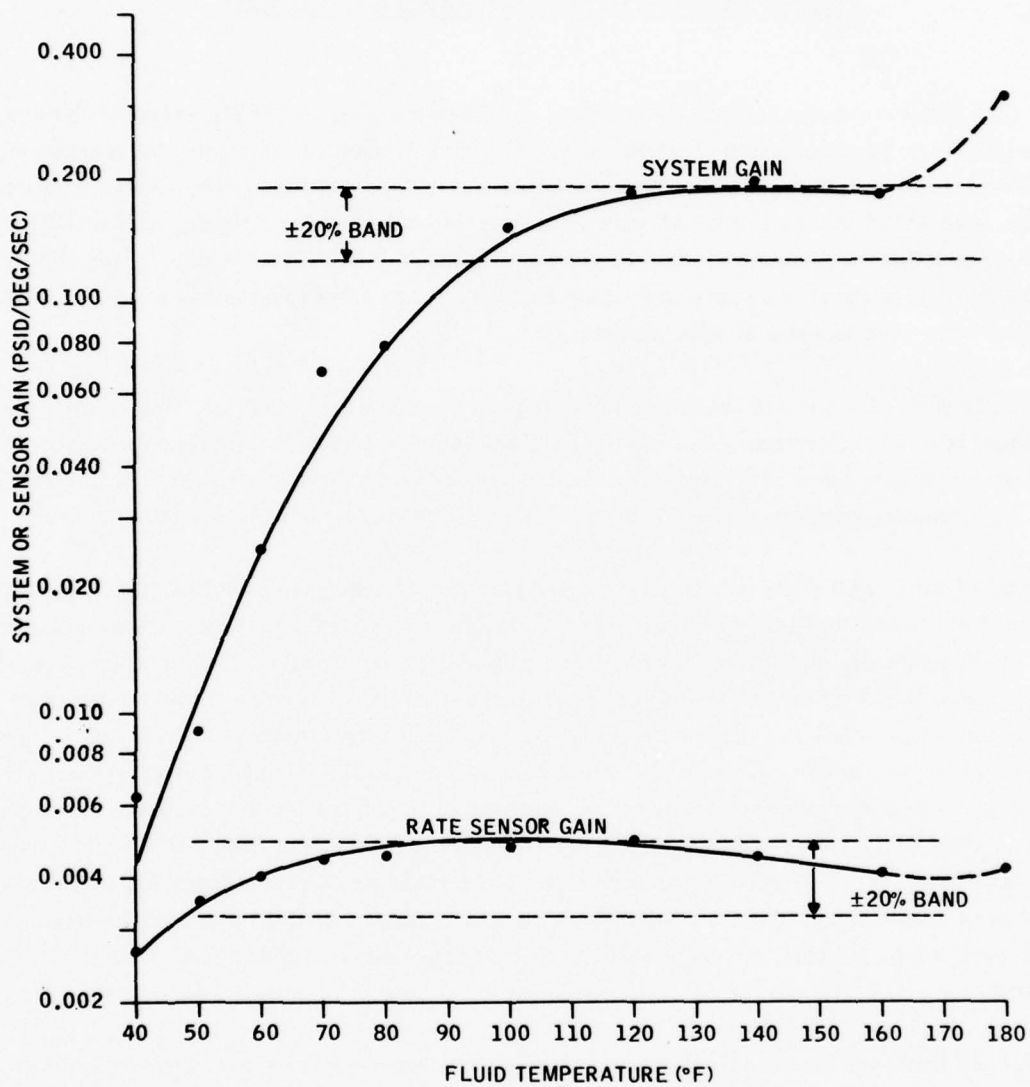


Figure 11. YG1143 System Standard Amplifiers Baseline Test - Rate Sensor and System Gain

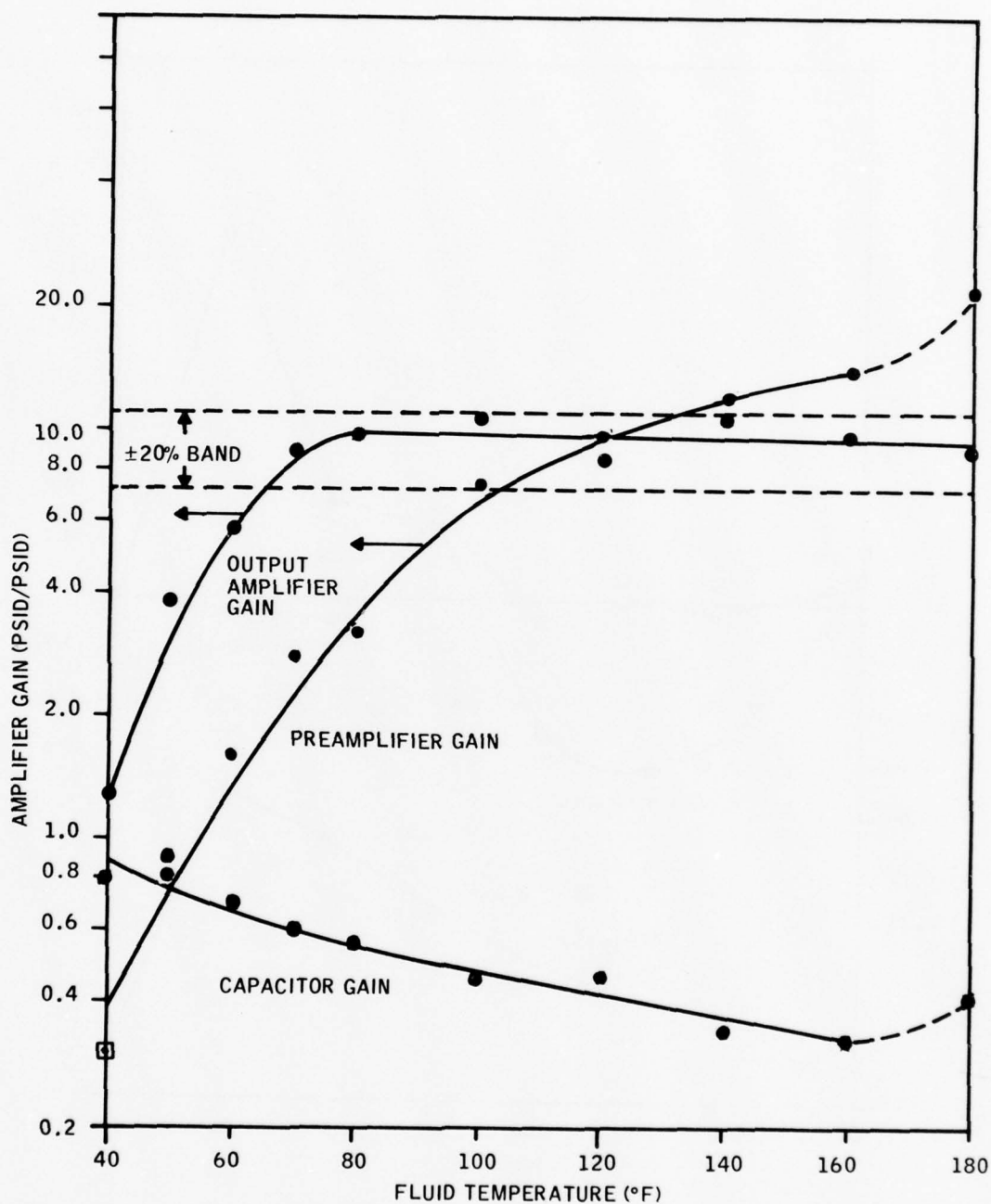


Figure 12. YG1143 Component Gains as a Function of Fluid Temperature - Standard Amplifiers.

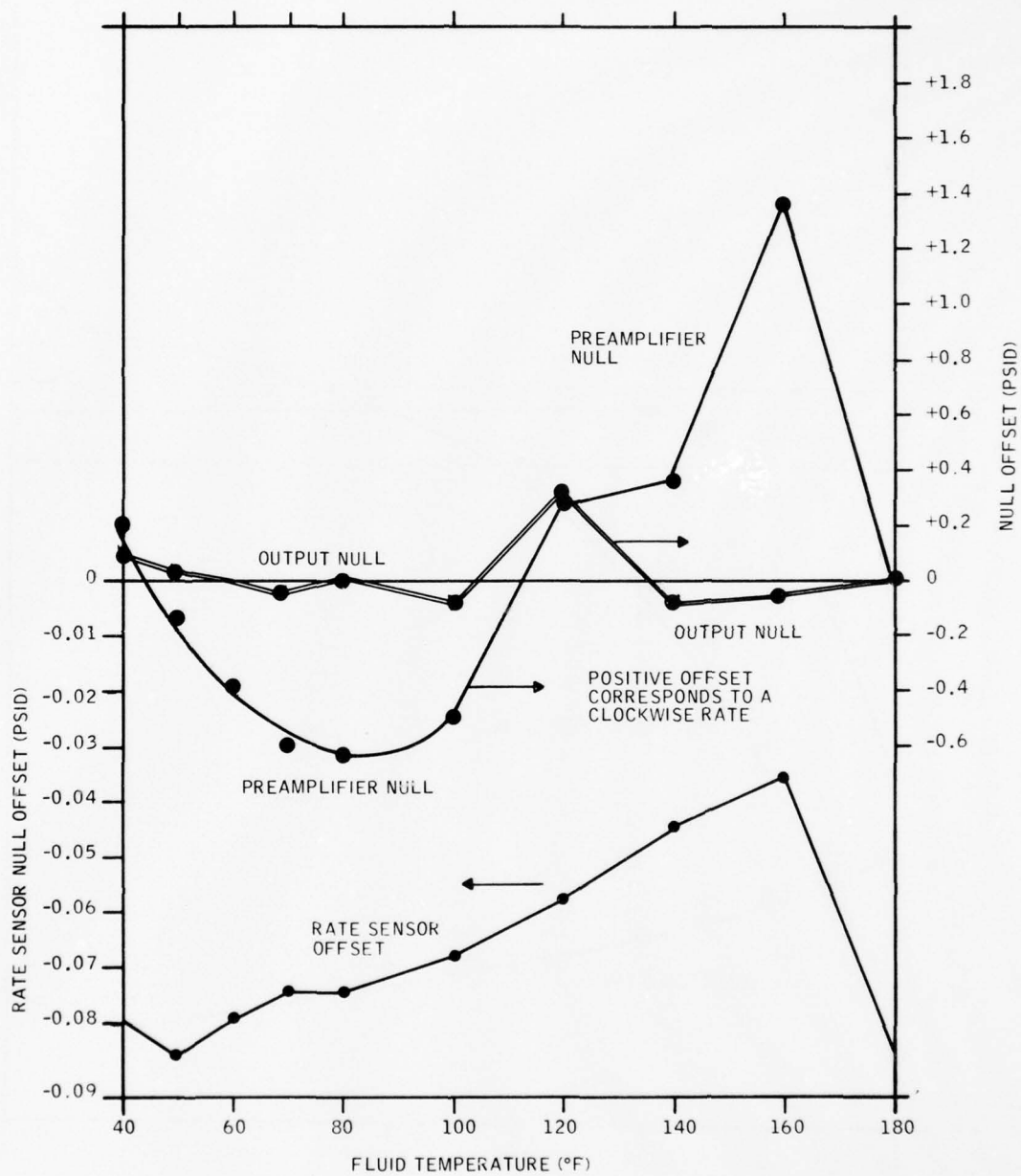


Figure 13. YG1143 System with Standard Amplifiers Baseline Test - Component and System Null Offset Characteristics.

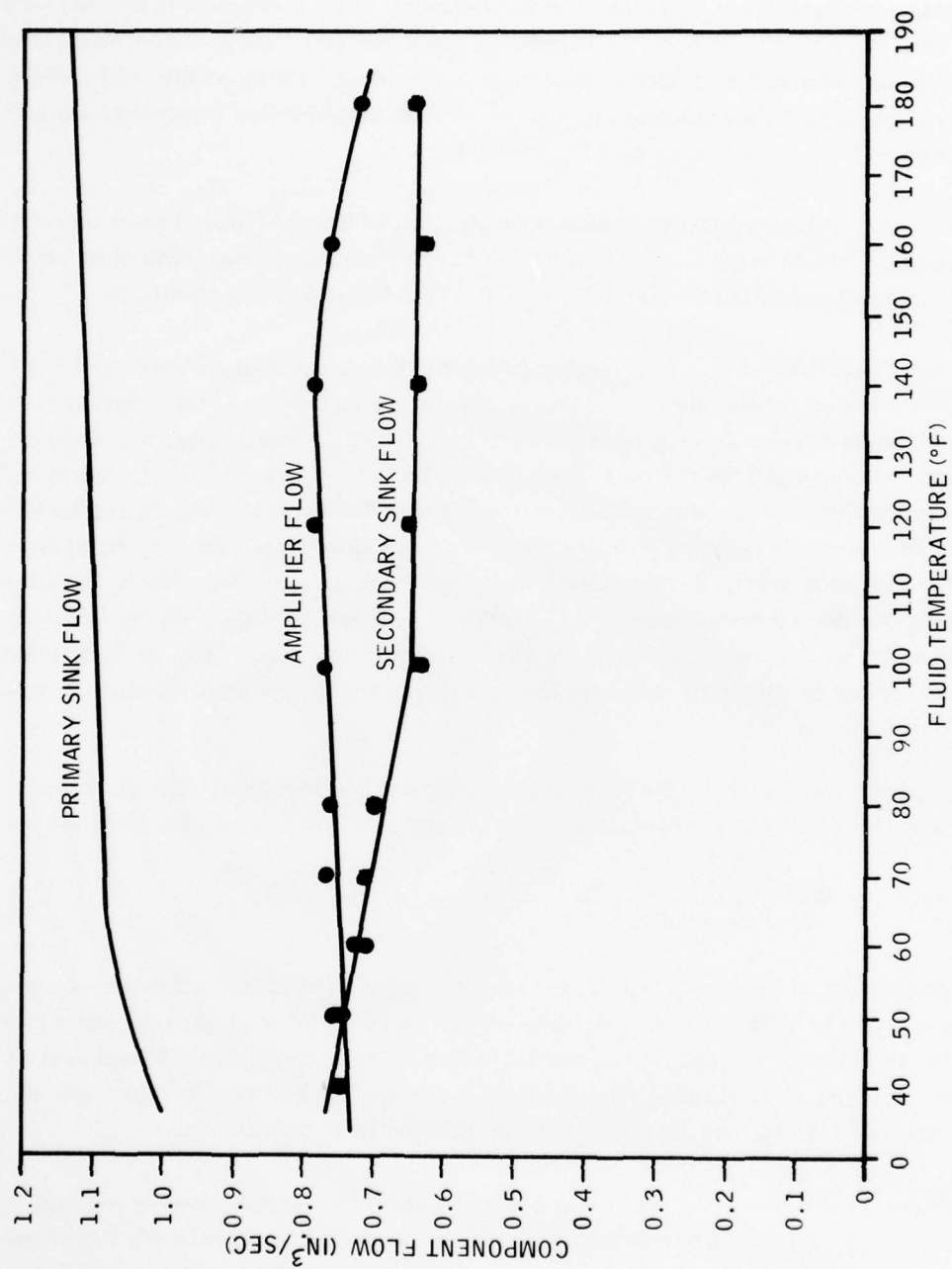


Figure 14. YG1143 System with Standard Amplifiers Baseline Test - Flow Split Versus Temperature.

Maintaining a constant flow split would be an improvement, and it is desirable to increase both primary sink and amplifier flow at the expense of secondary sink flow at cold temperature. Reduced primary sink and amplifier flows at high temperature have an additional benefit of reducing system noise under these conditions; however, if the amplifier flow is reduced too much, output range will fall below the ± 2 -psid requirement.

Figure 15, system frequency response, indicates that the desired transfer function was achieved as a result of modifications to the baseline system. The effect of instrumentation transducers can be noted by the increased attenuation and phase shift at the high-frequency conditions.

A series of tests was conducted on the baseline system with the standard amplifiers at 40°F to determine the potential of flow split compensation. The data of Figure 16 was taken with the secondary sink blocked (valve V₂ shown in Figure 5 closed). Valve V₅ was adjusted to change amplifier flow over the range 0.755 in.³/sec to 0.978 in.³/sec. Because system total flow is maintained constant by the flow control valve, rate sensor primary sink flow decreases when amplifier flow increases. This decrease in primary sink flow had only a slight effect on rate sensor gain; however, the resultant increase in amplifier flow greatly increased amplifier gain. There was no difficulty in obtaining the desired system gain of 0.15 psid/deg/sec at the 40°F temperature condition. The slope of the total system gain versus the amplifier flow curve is very high, indicating that it may be difficult to accurately maintain the gain within the ± 20 -percent tolerance at cold temperature.

Additional parametric data was taken with the standard amplifiers to evaluate their potential for compensation. Most fluidic amplifiers are sensitive to mass ratio, where mass ratio is defined as

$$\text{Mass Ratio} = \frac{\text{total control port flow}}{\text{power nozzle flow}} \quad (4)$$

Direct measurement of mass ratio was impractical; however, a qualitative indication of mass ratio was obtained by measuring control pressure level. Matching between the rate sensor and preamplifier is a primary concern, as it affects loading on the rate sensor pickoff as well as mass ratio to the amplifier. Compensation techniques that vary the flow between the rate sensor and amplifier cascade will also vary the pressure levels between these components.

The techniques used to obtain the parametric data of Figure 17 can be understood by referring to Figure 5. Flows Q₁, Q₂, and Q₃ were held constant during these tests; if valve V₃ was closed slightly, valve V₅ was opened to return Q₃ to its original value. Normal direction of signal flow is from the rate sensor pickoff to the control ports of amplifier A₁, resulting in a positive mass ratio.

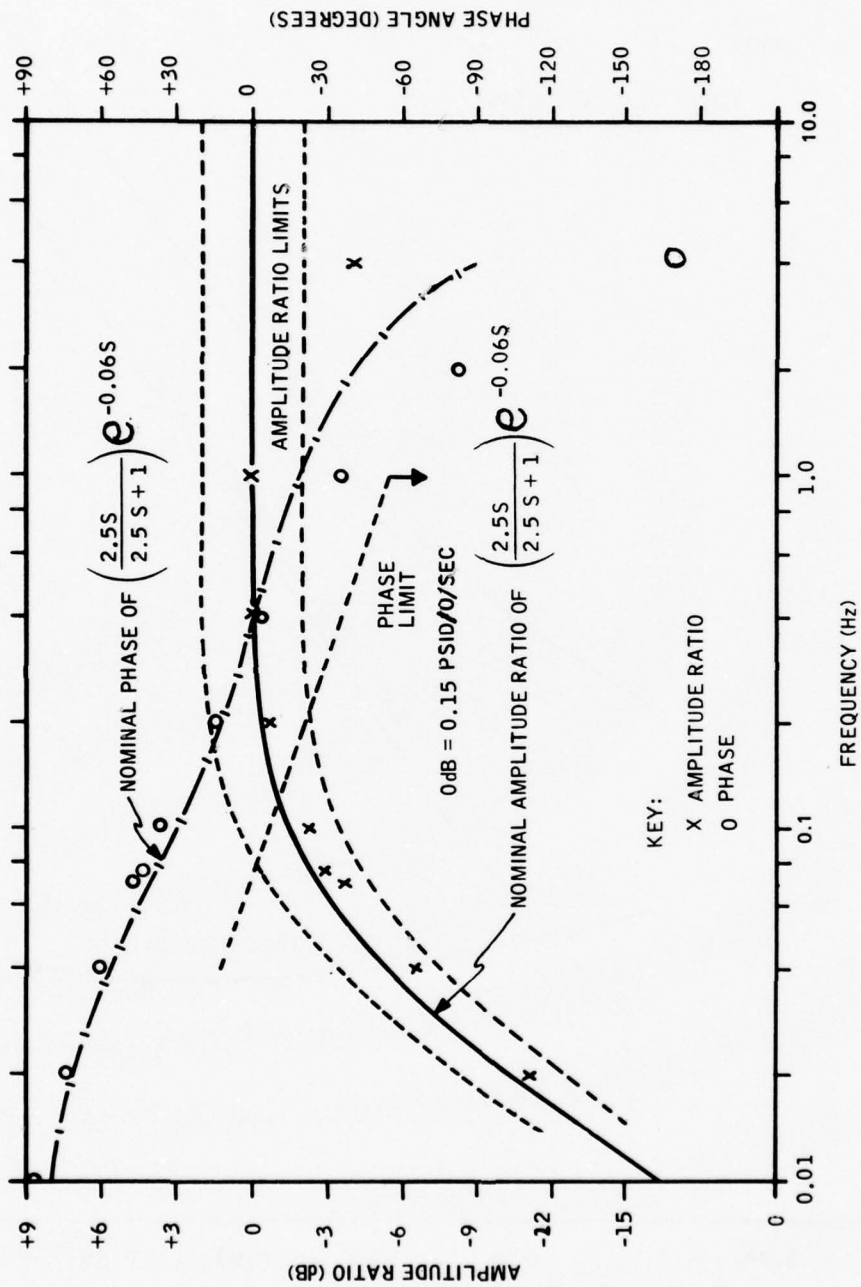


Figure 15. Baseline System with Standard Amplifiers Baseline Test - 120°F Frequency Response.

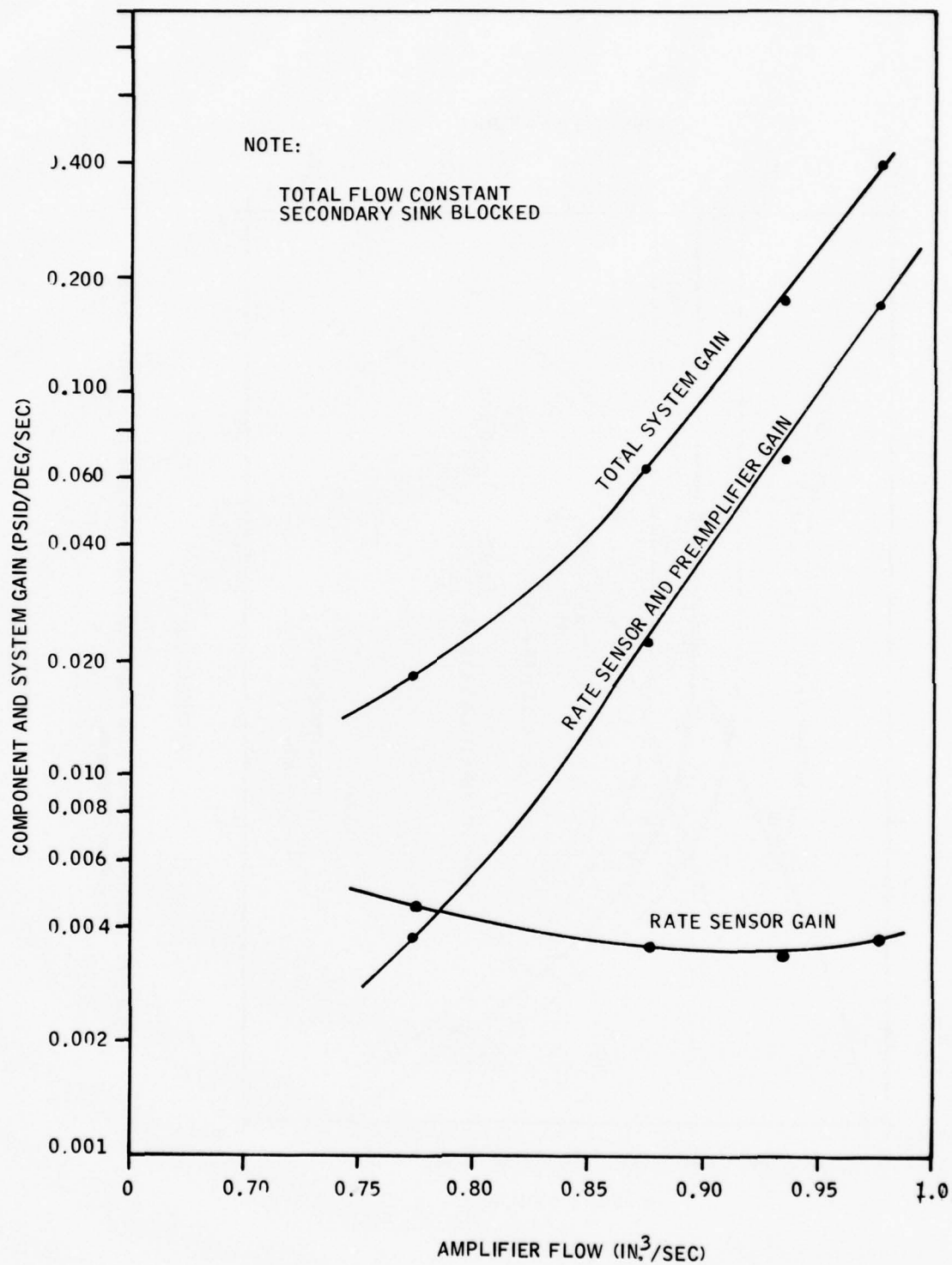


Figure 16. YG1143 System with Standard Amplifiers — Low Temperature Parametric Investigation (40°F)

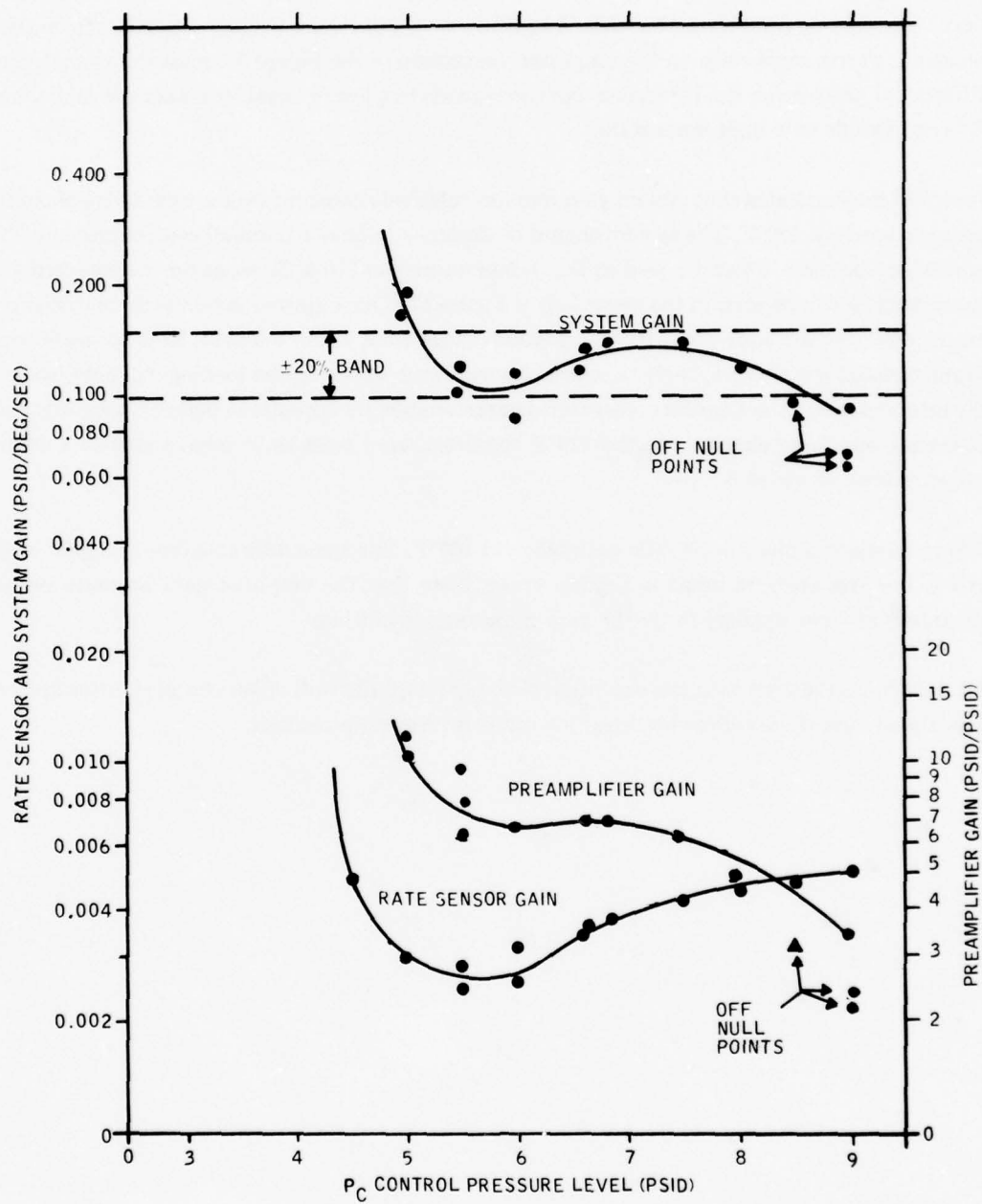


Figure 17. System Gains as a Function of Control Pressure Level — Standard Amplifiers, 120°F, $Q_A = 0.575 \text{ in.}^3/\text{sec}$

If valve V_3 is closed, the back pressure on the amplifiers will increase, reducing the amount of signal flow coming from the rate sensor. Amplifiers were sometimes back pressured sufficiently to cause a negative mass ratio on the amplifier. Inspection of the Figure 5 circuit shows that a low differential pressure on the P_C transducer corresponds to a low or negative mass ratio, and a high P_C corresponds to a high mass ratio.

Figure 17 demonstrates that system gain remains relatively constant over a wide range of control pressure levels at 120°F. The system should be designed to have a nominal control pressure level somewhere between 4.5 and 7 psid at this temperature condition. Reasons for the constant gain characteristic can be seen in the lower half of Figure 17. The amplifier is relatively insensitive to mass ratio over the equivalent control pressure range from 4.5 to 6.5 psid. Rate sensor loading characteristics are also relatively constant. Above 6 psid, however, the loading characteristics on the rate sensor and the amplifier mass ratio characteristics are opposite in polarity, partially compensating out these changes. At the 120°F condition, zero mass ratio corresponds to a control pressure level of about 3.5 psid.

Figure 18 shows similar mass ratio data taken at 180°F. The same desirable constant gain region exists, but the pressure range is slightly lower. Note that the amplifier gain becomes infinite (bistable) at what appears to be the zero mass ratio condition.

All data in this section with the exception of the preamplifier null offset characteristics indicate that the standard amplifiers are ideal for temperature compensation.

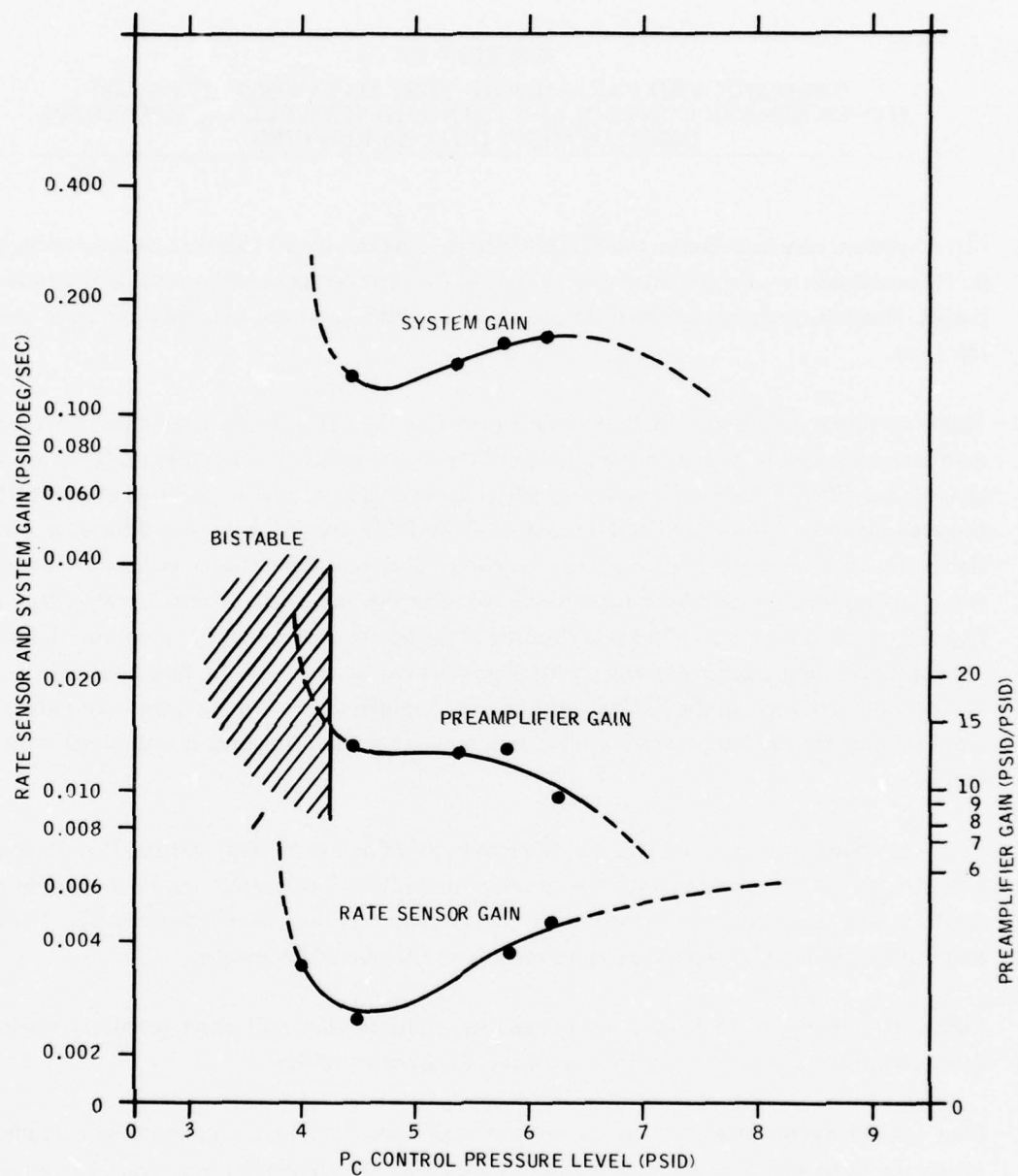


Figure 18. System Gains as a Function of Control Pressure Level — Standard Amplifiers, 180°F, $Q_A = 0.578 \text{ in.}^3/\text{sec}$

SECTION IV
BASELINE AND PARAMETRIC TEST DATA ON THE YG1143
HYSAS SENSOR CONTROLLER USING HONEYWELL INDEPENDENT
DEVELOPMENT (I.D.) AMPLIFIERS

I.D. amplifiers were installed on the YG1143 system using the adapter blocks discussed in Section II. This controller was calibrated at 120°F, and the frequency response shown in Figure 19 was obtained. Nominal performance with the standard amplifiers and the I.D. amplifiers was nearly identical.

Figure 20 shows system gain and rate sensor gain with the I.D. amplifiers installed. Rate sensor gain increases rapidly with increasing temperature as the result of an apparent interaction with the I.D. amplifiers, which appear to be approaching the zero mass ratio condition at about 125°F fluid temperature. Attempts to null the system above 130°F showed that it was bistable due to infinite gain over the center portion of the gain curve. This condition could have been corrected by reducing amplifier cascade back pressure by reducing the impedance of resistors R₁₈, R₁₉, and R₂₂ (Figure 5). Substantial effort was required in the operational suitability program (Reference 1) to optimize these resistors for the standard amplifiers. Parametric data, discussed later in this chapter, was obtained on the system with the I.D. amplifiers to determine if these amplifiers are more suitable for the temperature compensation program than the already optimized standard amplifiers.

Figure 21 shows capacitor and I.D. amplifier gains as a function of temperature. Performance is very similar to that obtained with the standard amplifiers. The output amplifier cascade with feedback was affected less by temperature change than was the preamplifier cascade. The I.D. amplifiers appear to be somewhat more sensitive to temperature change.

Figure 22, component null offset characteristics, indicate that null offset problems would be greater with the I.D. amplifiers than with the standard amplifiers.

Flow split characteristics between the primary sink, secondary sink, and amplifier cascade are nearly the same with the I.D. amplifiers as they are with the standard amplifiers. Comparison of Figure 23 data with that in Figure 14 indicates that the longer power nozzle on the I.D. amplifiers does not result in a greater reduction in amplifier flow at cold temperature.

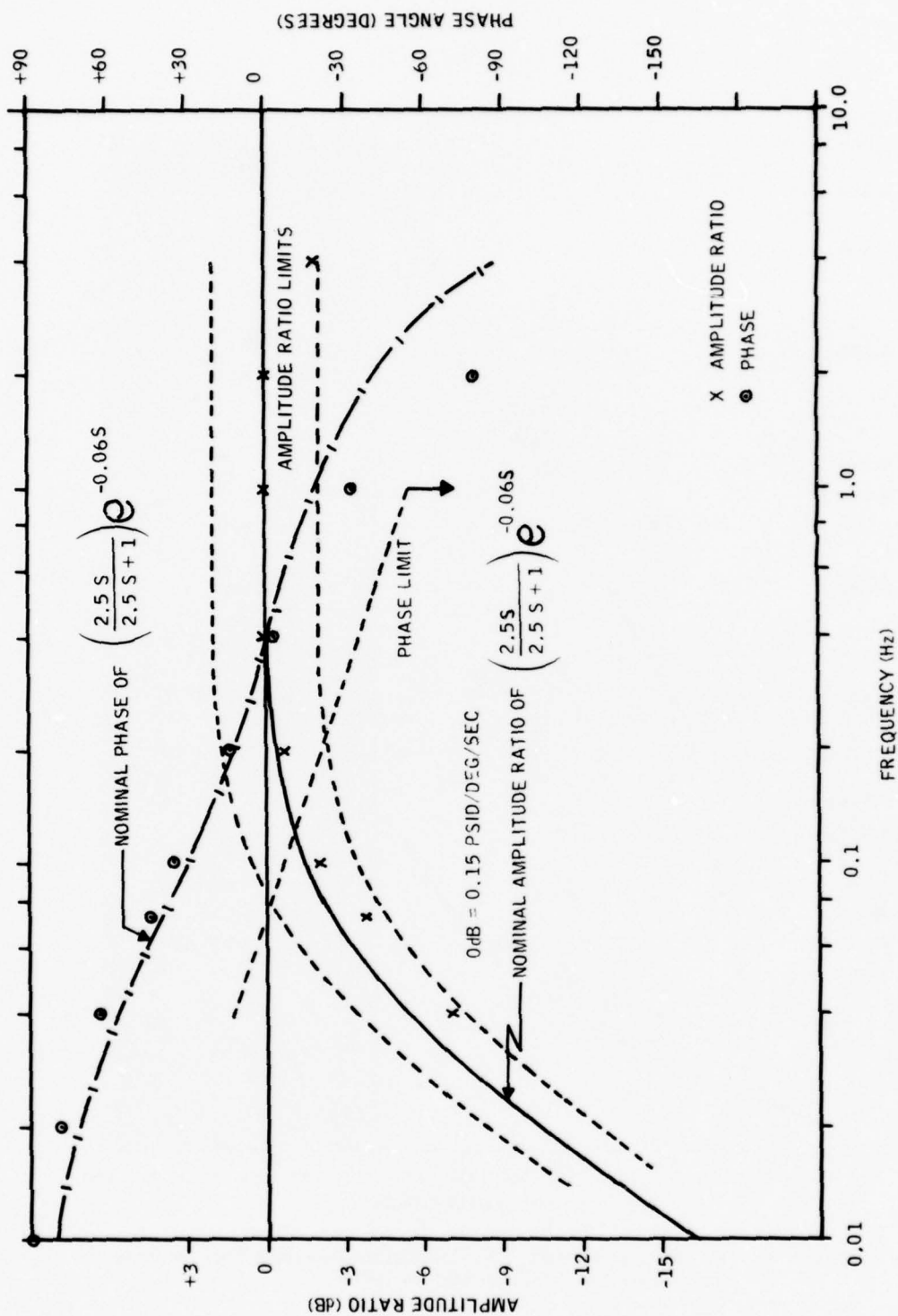


Figure 19. YG1143 System with I.D. Amplifiers Baseline Test - 120°F
Frequency Response.

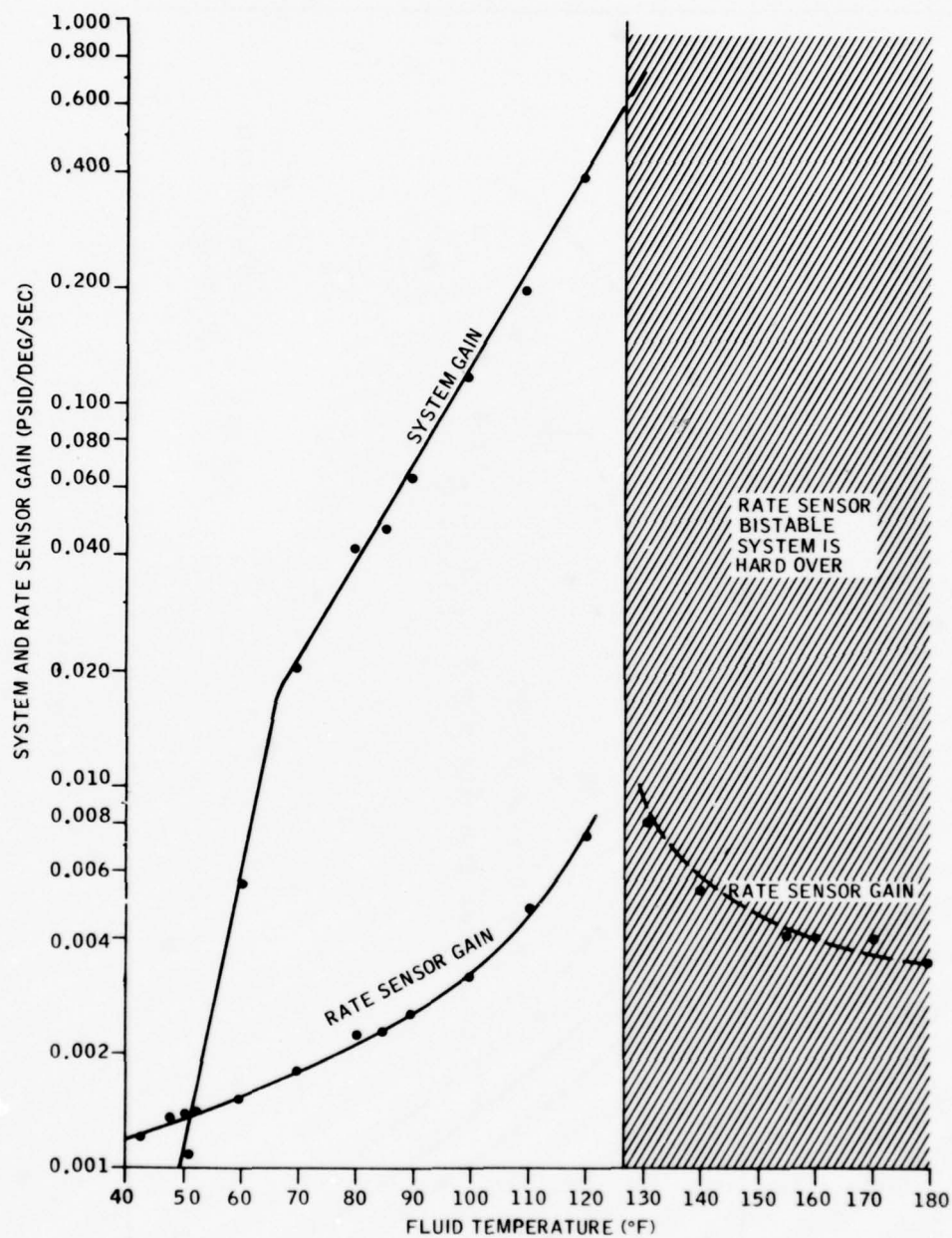


Figure 20. YG1143 System with I.D. Amplifiers Baseline Test — Rate Sensor and System Gain (40° to 180°F)

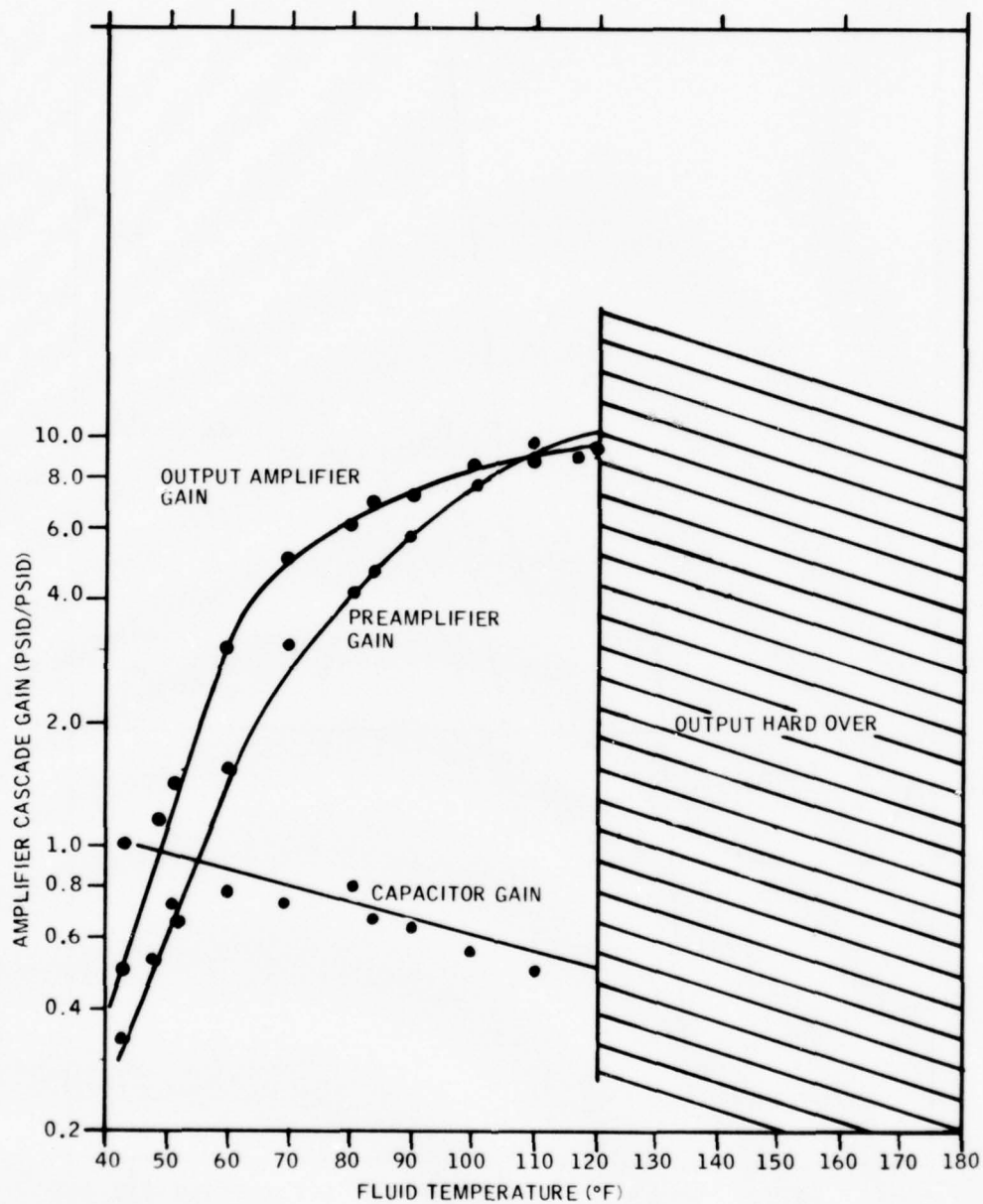


Figure 21. YG1143 System with I.D. Amplifiers Baseline Test — Component Gain Characteristics (40° to 180°F)

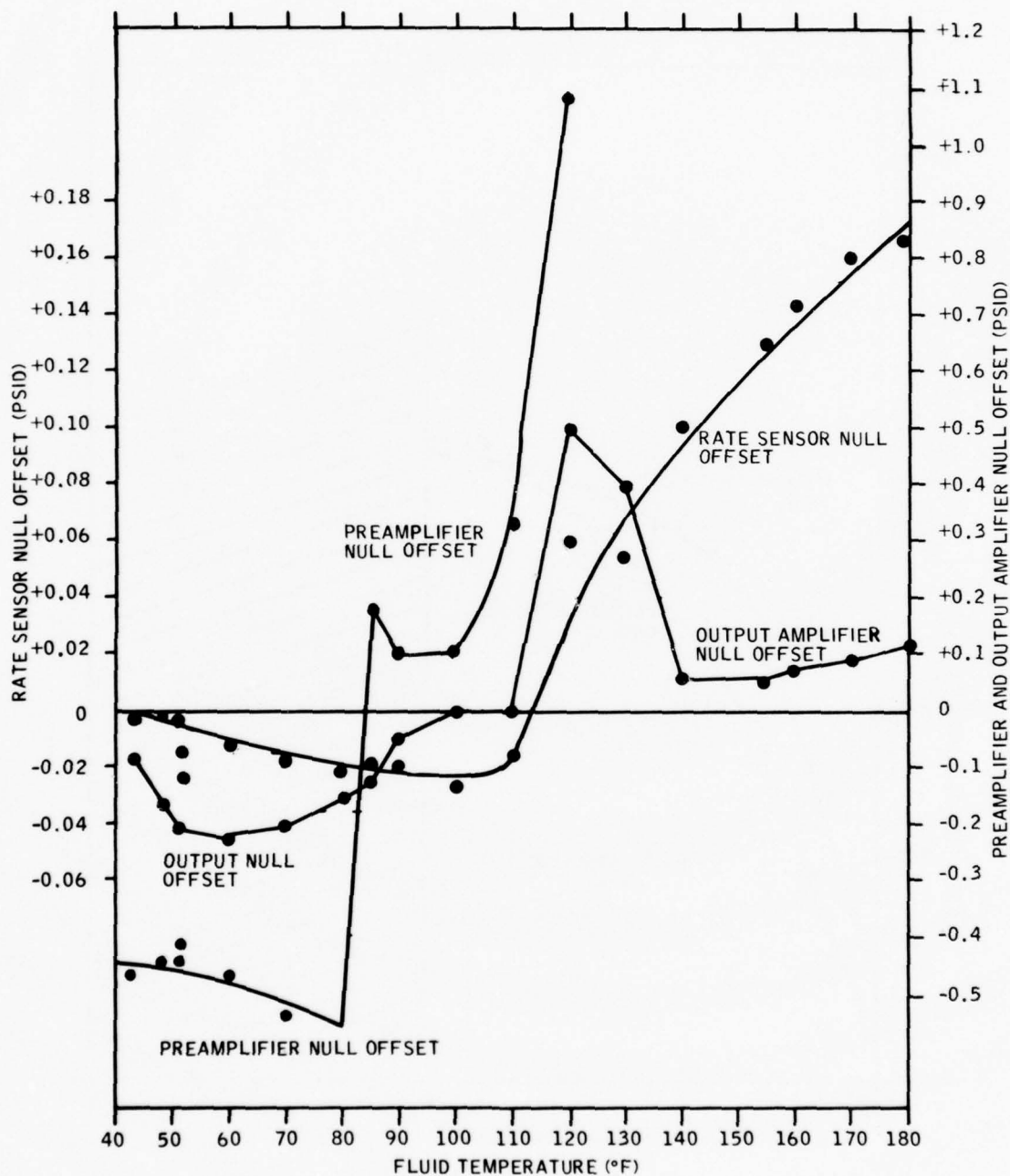


Figure 22. YG1143 System with I.D. Amplifiers Baseline Test — Null Offset Characteristics (40° to 180°F)

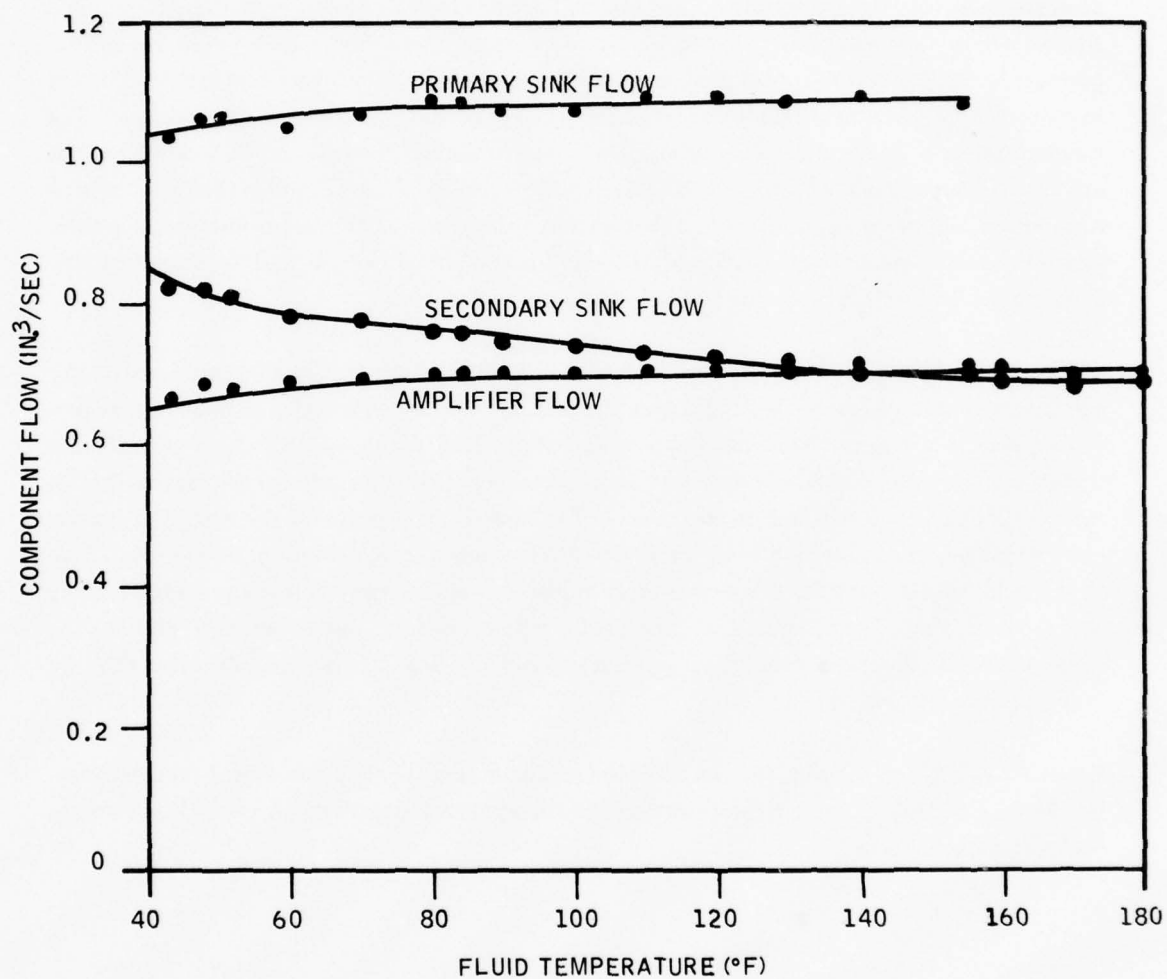


Figure 23. YG1143 System with I.D. Amplifiers - Flow Split Versus Temperature.

Parametric data was obtained at 40°F to investigate potential compensation problems with the I.D. amplifiers. The data of Figure 24 was taken at a constant control pressure level of 10 psid. It should be noted that the required gain of 0.15 psid/deg/sec could not be obtained at this control pressure level. The data of Figure 25 was taken at a constant amplifier flow of 1.02 in.³/sec, and the secondary sink was closed off completely. System gain was increased by reducing control pressure level. Maintaining adequate preamplifier null at 40°F was difficult, and it was necessary to reduce supply flow to obtain an unsaturated reading at the 3-psid control pressure level. The range of the rate sensor null offset adjust block is very limited, and partial disassembly of the system to change resistors R₃, R₄, or R₅ (Figure 5) is too laborious for efficient gathering of data. A comparison of Figures 24 and 25 shows that an adequate gain at 40°F can be obtained at a point where the control pressure level is 5 psid, the amplifier flow is 1.1 in.³/sec, and the secondary sink flow is zero. Null offset problems prevented testing in this area.

The parametric data of Figure 26, which was taken at 120°F, shows that system gain is extremely sensitive to control pressure level and that there is no constant gain region similar to that previously shown in Figure 17 for the standard amplifiers. Rate sensor loading characteristics and amplifier mass ratio characteristics shown at the bottom of Figure 26 indicate the reasons for this extreme sensitivity to control pressure level. The wide control ports on the amplifier greatly reduce rate sensor gain at high control pressure levels where a large amount of flow is taken from the pickoff. Rate sensor gain increases sharply at low control pressure levels where pickoff loading is greatly reduced. The preamplifier gain change with respect to control pressure level has the same polarity as the rate sensor gain change, and these effects add rather than cancel as they did with the standard amplifiers.

Parametric data comparisons indicate that the standard amplifier is better suited for compensation than is the I.D. amplifier. Therefore, use of the standard amplifiers for the YG1143 system was recommended.

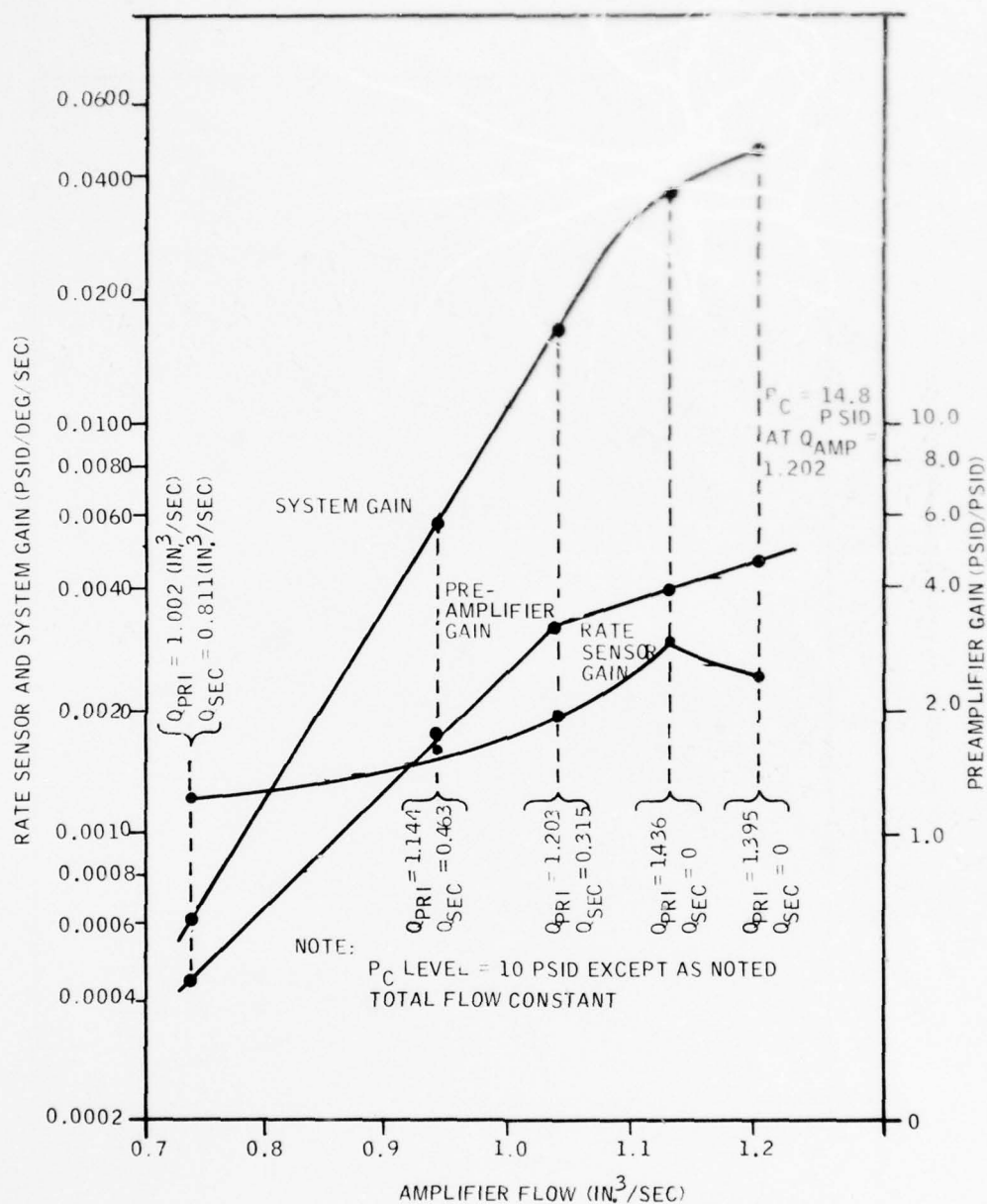


Figure 24. YG1143 System with I.D. Amplifiers - Low Temperature Parametric Investigations (40°F).

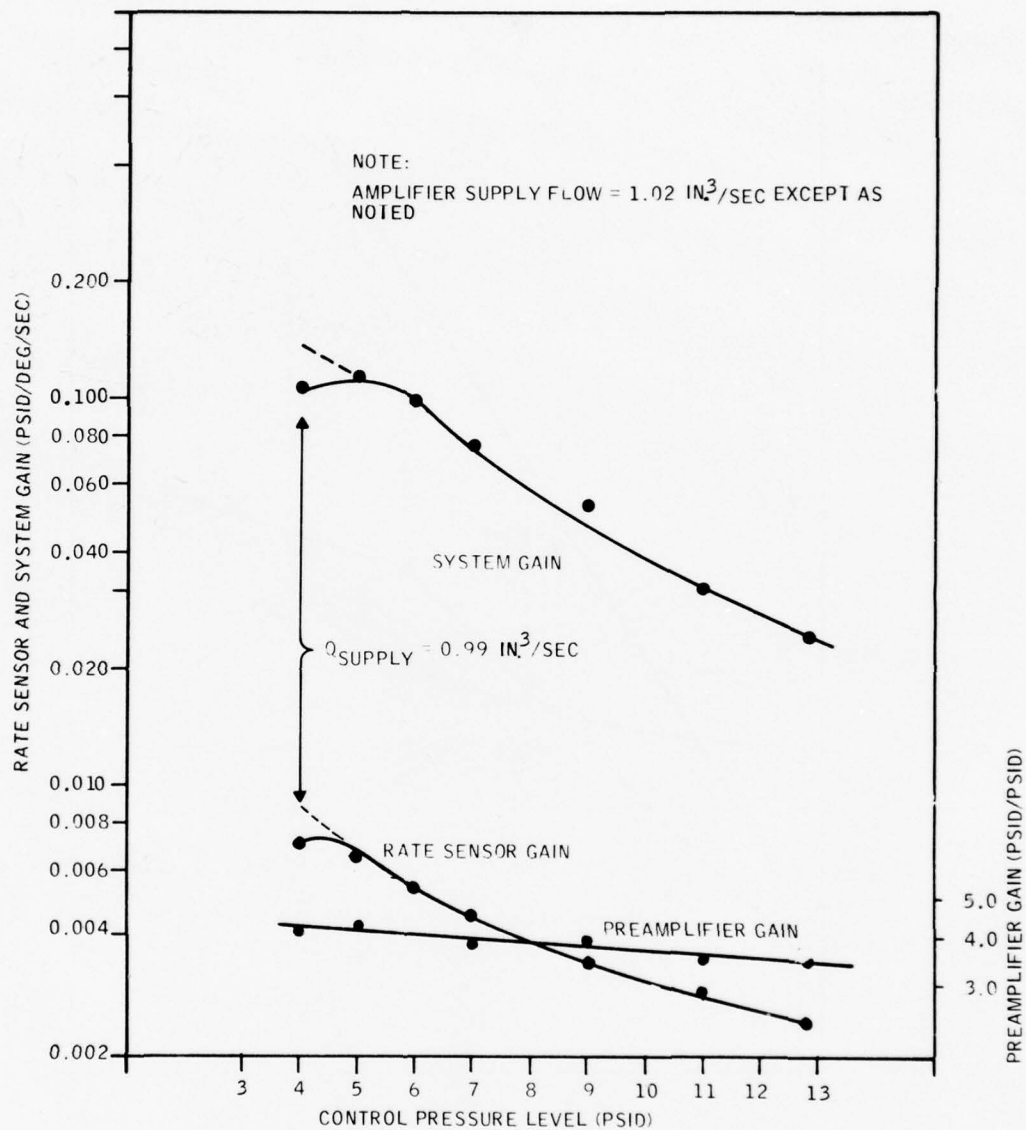


Figure 25. System Gains as a Function of Control Pressure Level — I.D. Amplifiers, 40°F, $Q_A = 1.02 \text{ in}^3/\text{sec}$

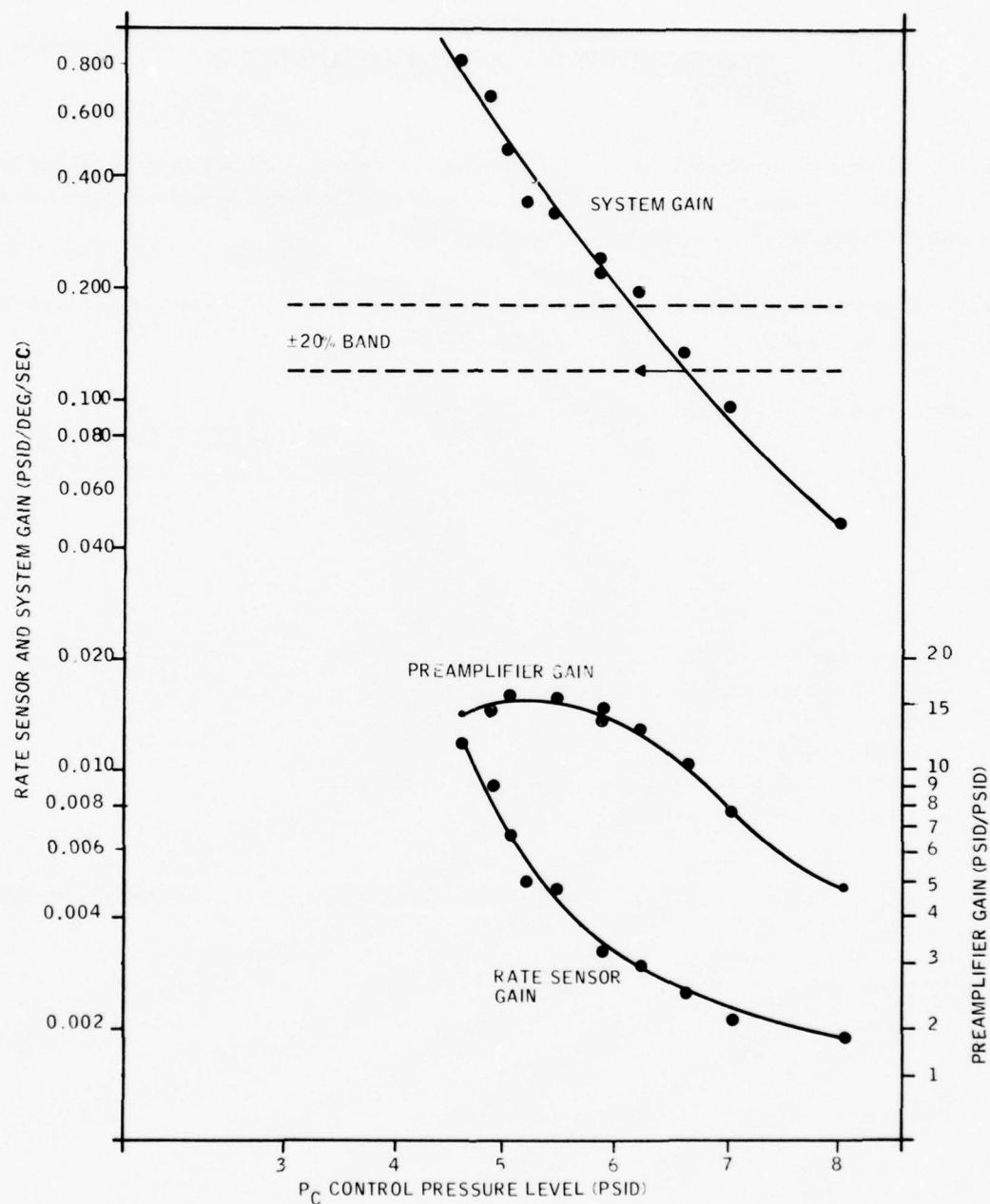


Figure 26. System Gains as a Function of Control Pressure Level —
I.D. Amplifiers, 120°F, $Q_A = 0.753 \text{ in.}^3/\text{sec}$

SECTION V

TEMPERATURE COMPENSATION ANALYSIS

Parametric data demonstrated the potential to compensate the YG1143 system by modifying the flow split between components as a function of temperature. The first step in the analysis was to define the characteristics of the various parallel flow paths.

Figure 27 shows the various hydraulic flow paths and their resistances. All flows, except the total flow, vary significantly as a function of fluid temperature.

Pressure drop across a restrictor has the characteristic

$$\Delta P = K_v Q + B Q^2 \quad (5)$$

where:

ΔP = pressure drop, psid

K = viscosity sensitive resistance coefficient $\frac{\text{lb sec}^2}{\text{in.}^7}$

Q = hydraulic flow, in.³/sec

B = sharp-edged orifice coefficient, lb-sec²/in.⁸

ν = fluid viscosity, centistokes

The viscosity sensitive coefficient is a function of restrictor geometry. For a rectangular channel, this coefficient is

$$K = \frac{1.325 \times 10^{-6} \ell}{C^3 W \left(\frac{W}{C + W} \right)^2} \quad (6)$$

For a square channel, this coefficient is reduced to:

$$K = \frac{5.3 \times 10^{-6} \ell}{W^4} \quad (7)$$

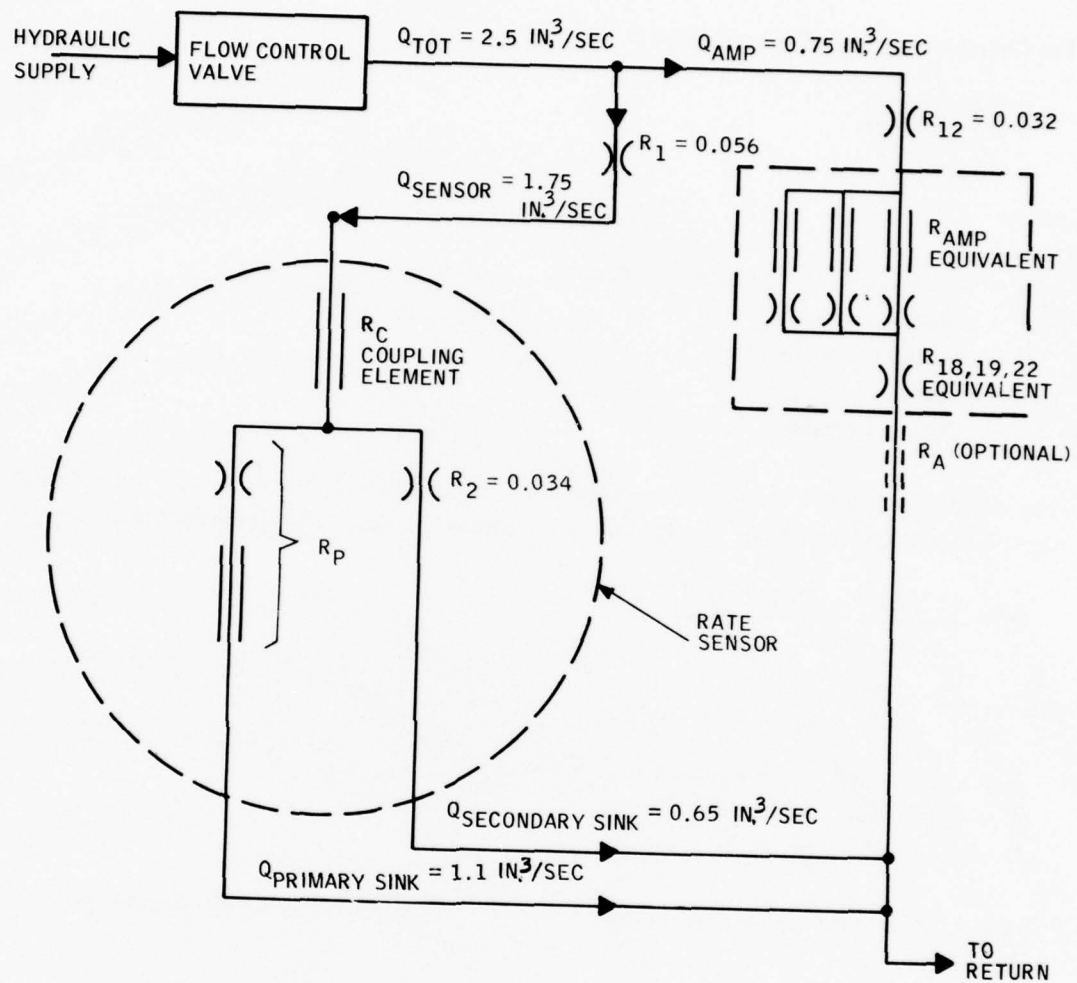


Figure 27. Resistances in Hydraulic Flow Paths.

For a circular channel this coefficient is also

$$K = \frac{5.3 \times 10^{-6} \ell}{D^4} \quad (8)$$

where:

K = viscosity sensitive resistance coefficient, $\frac{\text{lb sec}^2}{\text{in.}^7}$
 ℓ = channel length, in.
 C = channel height, in.
 W = channel width, in.
 D = channel diameter, in.

The sharp-edged orifice coefficient is a function of restrictor cross-sectional area, only because variations in discharge are not included in this simplified analysis. This coefficient is defined as:

$$B = \frac{9.5 \times 10^{-5}}{A^2} = \frac{1.524 \times 10^{-4}}{D^4} \quad (9)$$

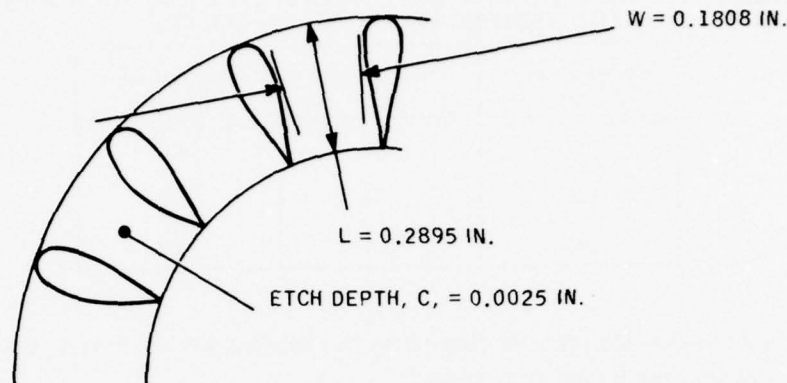
where:

B = sharp-edged orifice coefficient, $\text{lb-sec}^2/\text{in.}^8$
 A = orifice cross-sectional area, in.^2
 D = orifice diameter, in.

Characteristics of the rate sensor supply resistor, R_1 , using Equations 9 and 5 and a flow of 1.75 in.³/sec are

$$B = 15.5 \frac{\text{lb-sec}^2}{\text{in.}^8}, \quad \Delta P = 47.5 \text{ psid}$$

Figure 2 shows the rate sensor coupling elements. The sensor uses 34 elements, and each has 16 parallel restrictor paths. The pattern sketched below is etched 0.0025 in. deep.



Using Equation 6, the viscosity sensitive characteristic of each parallel path in each restrictor

$$K = \frac{1.325 \times 10^{-6} \mu}{C^3 W \left(\frac{W}{C+W} \right)^2} = 139.6 \quad (10)$$

The K for an entire coupling element is 1/16 of that given in Equation 10 or 8.72. Thirty-four elements in parallel reduce this K to 0.2565. Open area of the entire 34 coupling elements is

$$A = 0.1808 \times 0.2895 \times 0.0025 \times 16 \times 34 = 0.071 \text{ in.}^2 \quad (11)$$

This area is equivalent to an orifice 0.3 inch in diameter. Coefficient B for the coupling element stack using Equations 9 and 11 becomes 0.0188 lb-sec²/in.⁸. Using Equation 5, the pressure drop across the element with a flow of 1.75 in.³/sec through it becomes

$$\Delta P = \frac{0.2565 \nu \times 1.75 + 0.0188 (1.75)^2}{0.4637 \nu + 0.06} \text{ psid} \quad (12)$$

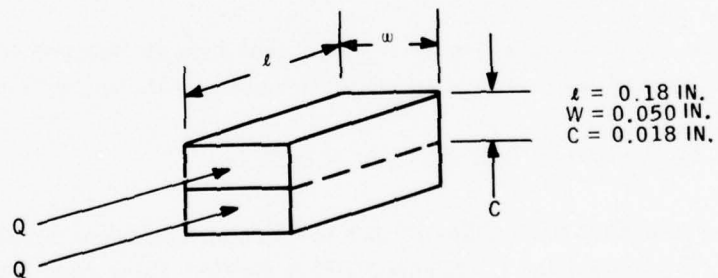
Table 1 gives the viscosity of MIL-H-5606 oil and the pressure drop across the coupling element at several temperatures.

TABLE 1. COUPLING ELEMENT PRESSURE DROP AS A FUNCTION OF OIL TEMPERATURE OR VISCOSITY

Temperature (°F)	Oil Viscosity (cs)	Element ΔP (psid)
40	30	14.0
120	11	5.2
180	6.4	3.0

This data shows that the pressure drop across the coupling element is very small, and it changes only 11 psid over the temperature range.

Pickoff geometry was simplified, as shown below, to permit the analysis of its pressure drop characteristics.



Each of the two parallel paths in this sensor has a calculated K of 1.5, resulting in a total K of 0.75. Total cross-sectional area is 0.0018 in.², resulting in a sharp-edged orifice coefficient of 29.3 lb-sec²/in.⁸. Characteristics of the pickoff are defined by the inclusion of these coefficients in Equation 5.

$$\Delta P_{\text{pickoff}} = 0.75\nu Q_p + 29.30Q_p^2 \quad (13)$$

If flow were maintained constant at 1.1 in.³/sec over the temperature range, the pressure drops listed in Table 2 would be obtained.

TABLE 2. RATE SENSOR PICKOFF PRESSURE DROP CHARACTERISTICS

Temperature (°F)	ν (cs)	$0.75\nu Q_p$ (psid)	$29.3Q_p^2$ (psid)	Total ΔP (psid)
40	30	24.8	35.5	60.3
120	11	9.1	35.5	44.5
180	6.4	5.3	35.5	40.8

The data of Table 2 shows that the rate sensor pickoff is primarily a sharp-edged orifice equivalent except when the fluid temperature is reduced below 40°F, where the viscosity sensitive drop begins to predominate.

Characteristics of the rate sensor secondary sink resistor are calculated to be

$$\Delta P = 114 Q_s^2 \text{ psid} \quad (14)$$

This results in a pressure drop of 48 psid whenever the flow is 0.65 in.³/sec.

Because pickoff and secondary sink have parallel paths, their pressure drops are equal and the sum of their flows are equal to the rate sensor flow. For a sensor flow of 1.75 in.³/sec,

$$\text{rate sensor flow} = \text{pickoff flow} + \text{secondary sink flow}$$

$$Q_R = 1.75 = Q_P + Q_S \quad (15)$$

Setting Equation 13 equal to Equation 14 yields

$$0.75\nu Q_P + 29.30Q_P^2 = 114Q_S^2 \quad (16)$$

A solution to Equations 15 and 16 is given in Table 3 for fluid at three different viscosity levels. Pressure drop was also calculated using Equation 14.

TABLE 3. CALCULATED PICKOFF AND SECONDARY SINK FLOW SPLIT CHARACTERISTICS WITHOUT COMPENSATION

Temperature (°F)	ν (cs)	Q_P in. ³ /sec	Q_S in. ³ /sec	ΔP (psid)
40	30	1.050	0.700	55.9
120	11	1.117	0.633	45.7
180	6.4	1.135	0.615	43.2

Calculated performance at the three temperature conditions given in Table 3 is based on the physical geometry of the rate sensor and the assumption that rate sensor flow is constant. This data compares very closely with the results obtained during testing of the baseline system as shown on Figure 14. Test conditions were more complex, as the amplifiers operating in parallel with the rate sensor caused the rate sensor flow rate to change slightly with respect to temperature. Characteristic impedance of the amplifier cascades including back pressure resistors R₁₈, R₁₉, and R₂₂ (not including supply resistor R₁₂, Figure 27) was calculated to be

$$\Delta P_{amp} = 1.3\nu Q_a + 14 Q_a^2 \quad (17)$$

Resulting pressure drops at a flow of 0.75 in.³/sec are given in Table 4.

TABLE 4. AMPLIFIER CASCADE PRESSURE DROP CHARACTERISTICS

Temperature (°F)	ν (cs)	$1.3\nu Q_a$ (psid)	$14Q_a^2$ (psid)	Total ΔP (psid)
40	30	29.3	7.9	37.2
120	11	10.7	7.9	18.6
180	6.4	6.2	7.9	14.1

Pressure drop across the 0.032-inch-diameter supply orifice at 0.75 in.³/sec flow is calculated using Equation 9 to be

$$\Delta P_{R_{12}} = \frac{1.5240 \times 10^{-4}}{(0.032)^4} \times (0.75)^2 = 81.75 \text{ psid} \quad (18)$$

Calculated characteristic impedances of the controller flow paths are summarized in Figure 28. Shown below each block is the component pressure drop at 120°F, using the calculated characteristic impedance and a typical flow. Typical flows were adjusted slightly from those shown in Figure 27 to have equal calculated pressure drops across parallel paths; i.e., because pressure drops across the primary and secondary sinks must be equal, the flow split was adjusted very slightly to obtain the balanced condition.

The parametric data presented in Section III showed that low temperature gain can be improved by greatly reducing secondary sink flow at cold temperature, while increasing both pickoff flow and amplifier flow. The opposite effect must occur at high temperature to prevent sensor and amplifier noise. This can be accomplished by replacing the sharp-edged orifice, R₂, in the secondary sink with an element that is substantially more sensitive to viscosity than the primary sink. Figure 29 shows the secondary sink compensating restrictor. The restrictor discs are like miniature coupling elements, which are 0.345 inch in diameter and 0.006 inch thick. Each disc has four channels; each channel has an average width of 0.10 inch, is 0.0975 inch long, and is etched to a depth, C, of 0.00325 inch. Substituting these dimensions into Equation 10 yields

$$K_{\text{channel}} = \frac{1.325 \times 10^{-6} \ell}{C^3 W \left(\frac{W}{C+W} \right)^2} = 40.12 \quad (19)$$

The minimum channel width of 0.075 inch was used rather than the average width of 0.10 inch in calculating the open area per channel, which is $2.4375 \times 10^{-4} \text{ in.}^2$.

The configuration of the secondary sink compensating restrictor used in the first compensation investigations consisted of a stack of 6 discs in series with a stack of 5 discs. The viscosity sensitive resistance coefficient for this combination of discs is

$$K = \frac{40.12}{4 \times 6} + \frac{40.12}{4 \times 5} = 3.7 \quad (20)$$

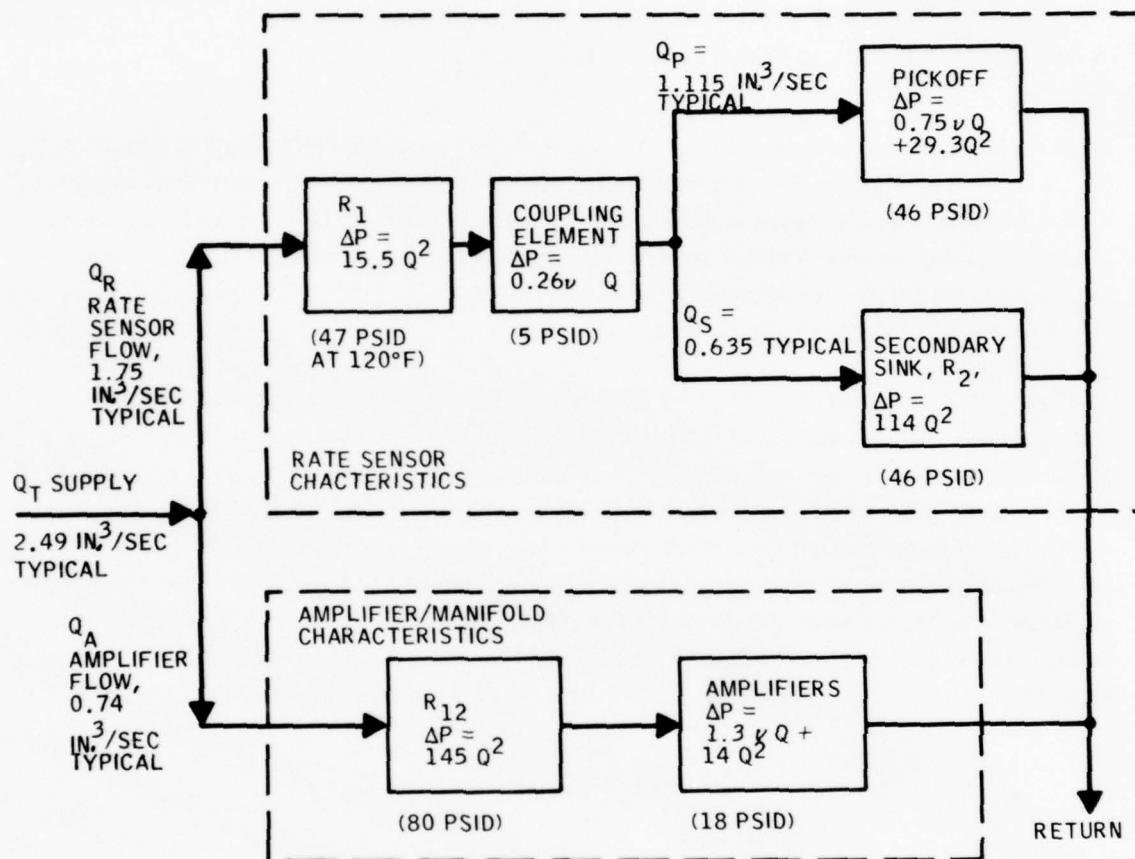


Figure 28. Flow Path Calculated Characteristic Impedances.

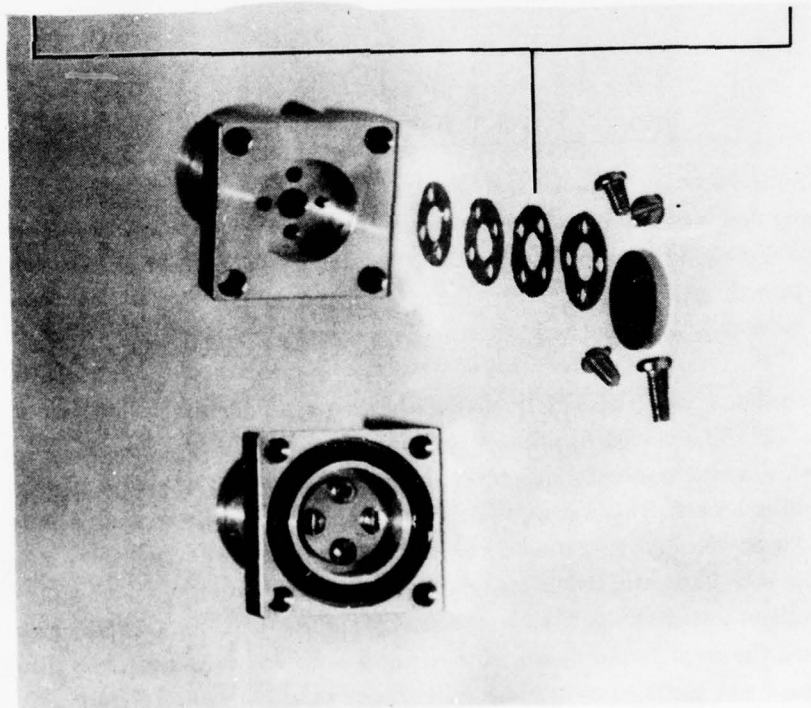
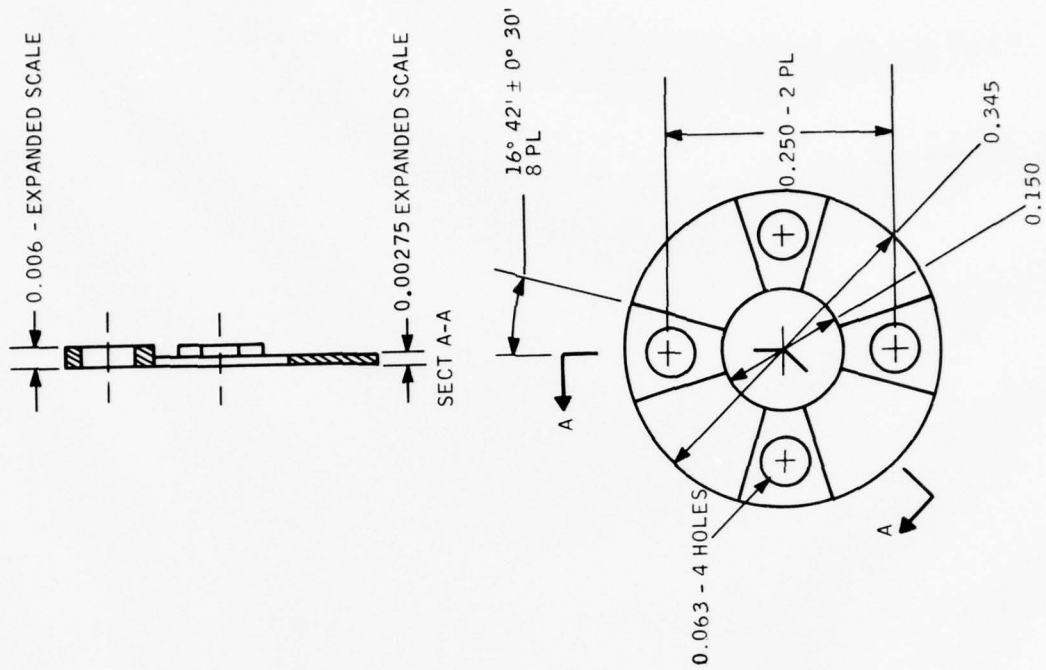


Figure 29. Temperature Compensation Element—Photograph and Schematic.

The sharp-edged orifice coefficient for this configuration of discs using Equation 9 is

$$B = \frac{9.5 \times 10^{-5}}{(4 \times 6 \times 2.4375 \times 10^{-4})^2} + \frac{9.5 \times 10^{-5}}{(4 \times 5 \times 2.4375 \times 10^{-4})^2} = 6.8 \quad (21)$$

Characteristics of the secondary sink with compensation is then defined using Equation 5 as

$$\Delta P_{\text{secondary sink}} = 3.7 \nu Q_s + 6.8 Q_s^2 \quad (22)$$

Flow split characteristics with the compensated secondary sink can be determined by setting pickoff pressure drop, Equation 13, equal to compensated secondary sink pressure drop, Equation 22, and solving this simultaneously with Equation 15. Results of these calculations are given in Table 5 for three different temperatures.

Table 5. Calculated Pickoff and Secondary Sink Flow Split Characteristics with Compensation

Temperature (°F)	ν (cs)	Q_p in. ³ /sec	Q_s in. ³ /sec	ΔP (psid)
40	30	1.17	0.58	66.5
120	11	0.97	0.78	35.7
180	6.4	0.87	0.88	26.2

The data of Table 5 does not include the effects of the parallel amplifier branch but assumes that total rate sensor flow is constant. In actual operation, the secondary sink will also cause amplifier flow to change slightly for the same reasons that it caused primary flow to change. When all factors are considered, secondary sink flow changes will be greater than shown, pressure drop changes will be slightly less, and primary sink flow changes will be less.

The parametric data given in Section III showed that changes in amplifier flow produced greater gain changes than did a change in primary sink flow. One method for increasing amplifier flow under cold temperature conditions is to make the rate sensor branch more sensitive to viscosity than the amplifier branch. This was partially accomplished with the secondary sink resistor. An inspection of Figure 28 shows that resistors R_1 and R_{12} , both sharp-edged orifices, are the dominant element in each flow path. Removing R_1 from the rate sensor flow path and replacing it with a viscosity sensitive restrictor would make the rate sensor flow path substantially more sensitive to viscosity than the amplifier flow path. In this program, R_1 was drilled out, and the rate sensor coupling element was modified to increase its viscosity sensitive pressure drop.

The number of discs in the coupling element was reduced to reduce the number of parallel flow paths and, therefore, increase its resistance to flow. Because the height of the element must remain fixed, spacer discs were fabricated to replace the elements removed. Figure 30 shows a coupling element with blank spacers.

The number of coupling elements was reduced from 34 to 6 in some tests and to 4 in other tests. Characteristics of these configurations can be calculated from data in Equations 5, 9, 10, and 11. Resultant pressure drop characteristics are

$$\Delta P_{6 \text{ elements}} = 1.45 \nu Q_R + 0.60 Q_R^2 \quad (23)$$

$$\Delta P_{4 \text{ elements}} = 2.18 \nu Q_R + 1.36 Q_R^2 \quad (24)$$

Pressure drop of these coupling elements at the conditions defined in Figure 28 is 30 psid for the six-element configuration and 46 psid for the four-element configuration. The increase in pressure drop due to fewer elements is less than the reduction in pressure drop due to the elimination of R_1 .

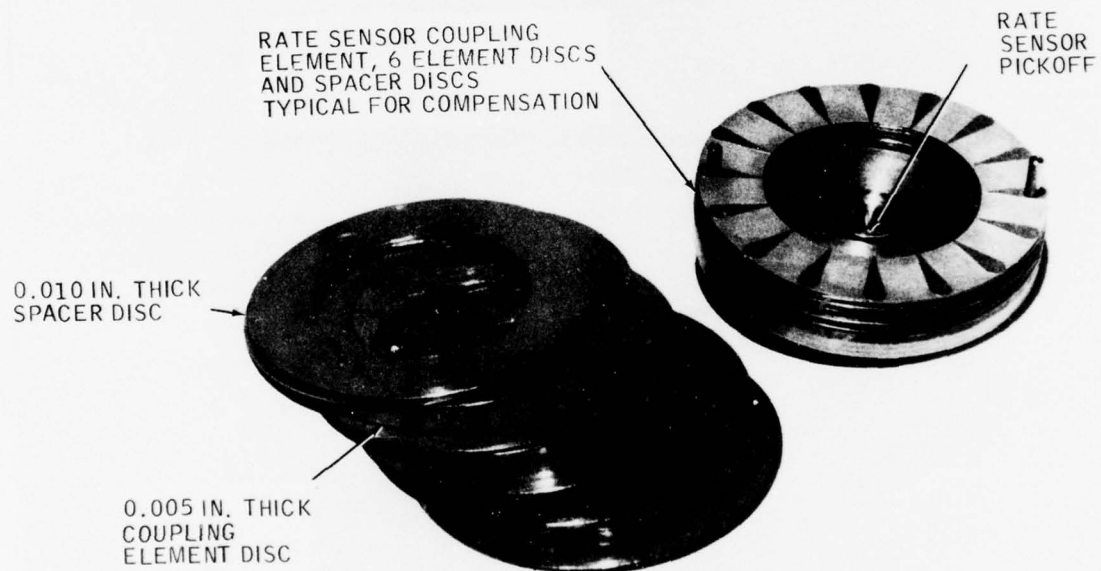


Figure 30. Coupling Element Modification.

SECTION VI

DEVELOPMENT TESTING

Development tests were performed on four compensation configurations. In all configurations, standard amplifiers were used, the rate sensor restrictor, R_1 , was removed, viscosity sensitive elements were used in the secondary sink, and the number of rate sensor coupling elements was reduced.

In Configuration one, six rate sensor coupling element discs with spacers and a secondary sink with six parallel discs in series with five parallel discs were used.

In Configuration two, a viscosity sensitive restrictor was added in the amplifier return line to reduce control pressure level and, thereby, improve mass ratio. Resistance of the secondary sink was increased by reducing the number of discs to five parallel discs in series with four parallel discs.

Configuration number three was the same as two except the adjustable restrictor in series with R_{12} was used to decrease amplifier flow by about 4 percent.

In Configuration four, the number of rate sensor coupling elements was reduced to four, the secondary sink configuration of five discs in series with four discs was retained, and the viscosity sensitive restrictor in the amplifier return line was removed.

Figure 31 shows system gain as a function of temperature for Configuration one. When compared to the baseline system, Figure 11, this configuration has improved low temperature gain by a factor of 5. Rate sensor gain characteristics were also improved. Configuration one component gains, Figure 32, show that the preamplifier gain (when compared to Figure 12) was improved the most. Null offset variations, Figure 33, are substantial, and the upper peak coincides with dip in the system gain curve. Most importantly, a comparison of Figure 34 with Figure 14 shows that the changes in flow for the rate sensor primary sink, amplifier cascade, and secondary sink all vary in the desired direction with respect to changes in fluid temperature.

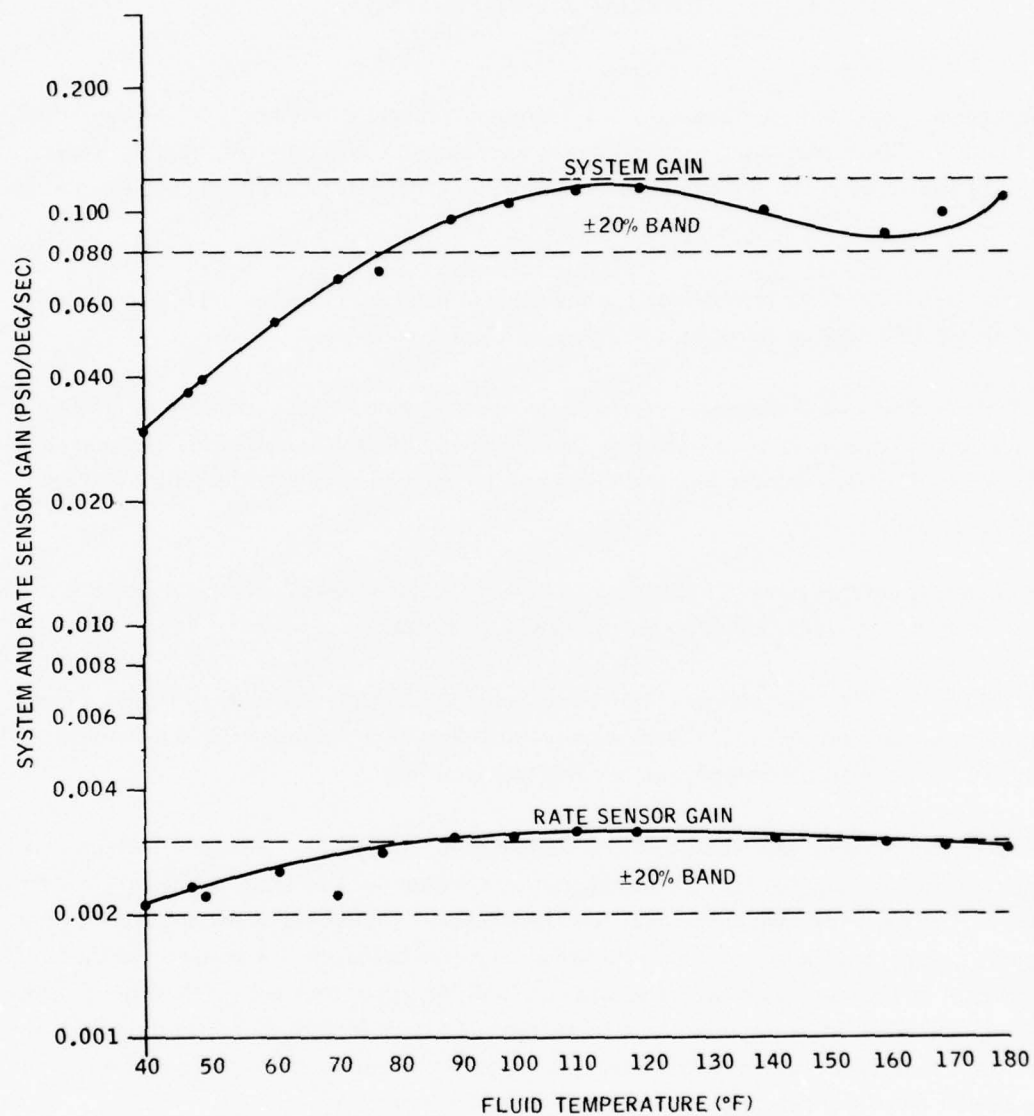


Figure 31. Configuration One System Gain Characteristics.

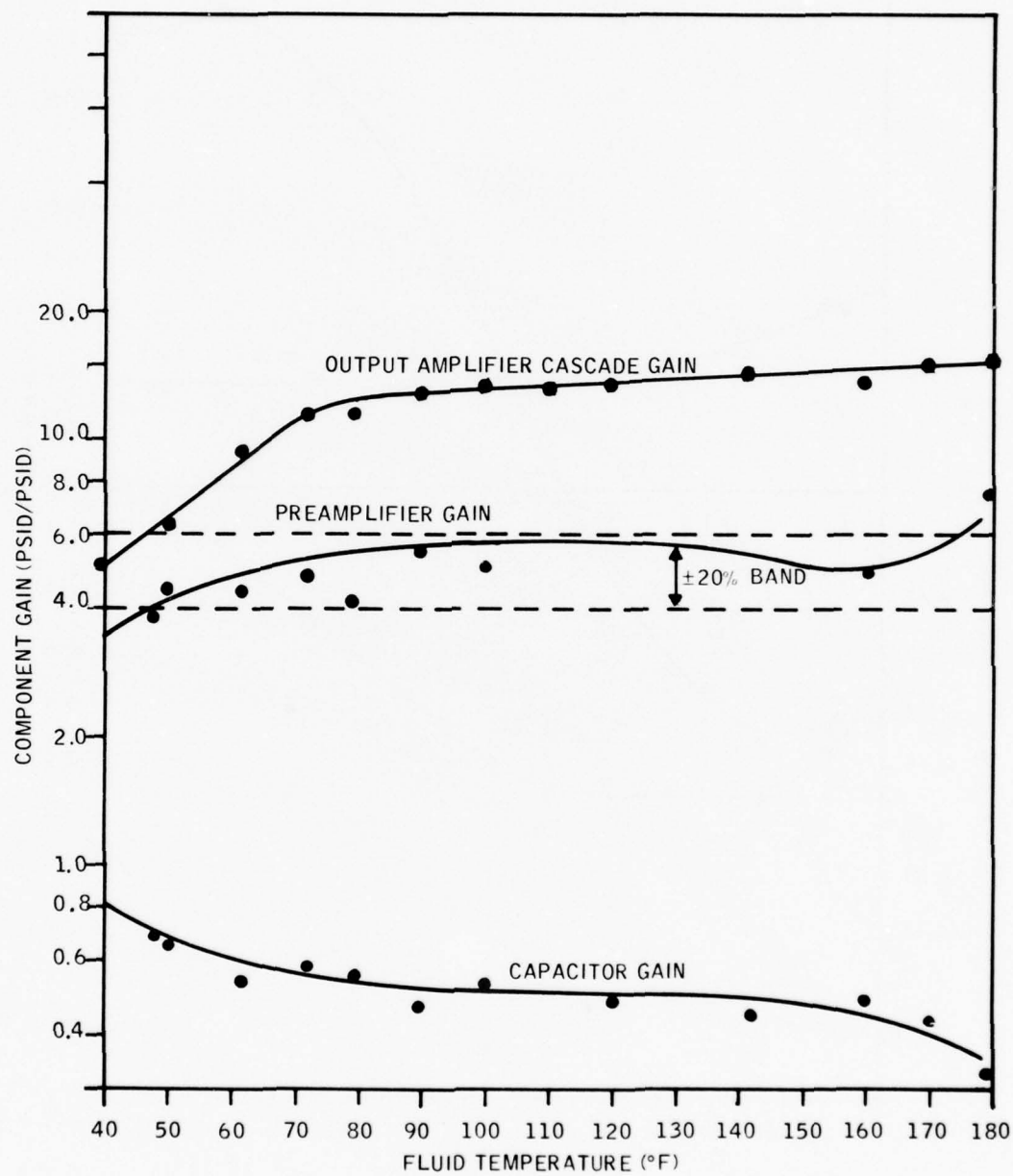


Figure 32. Configuration One Component Gain Characteristics.

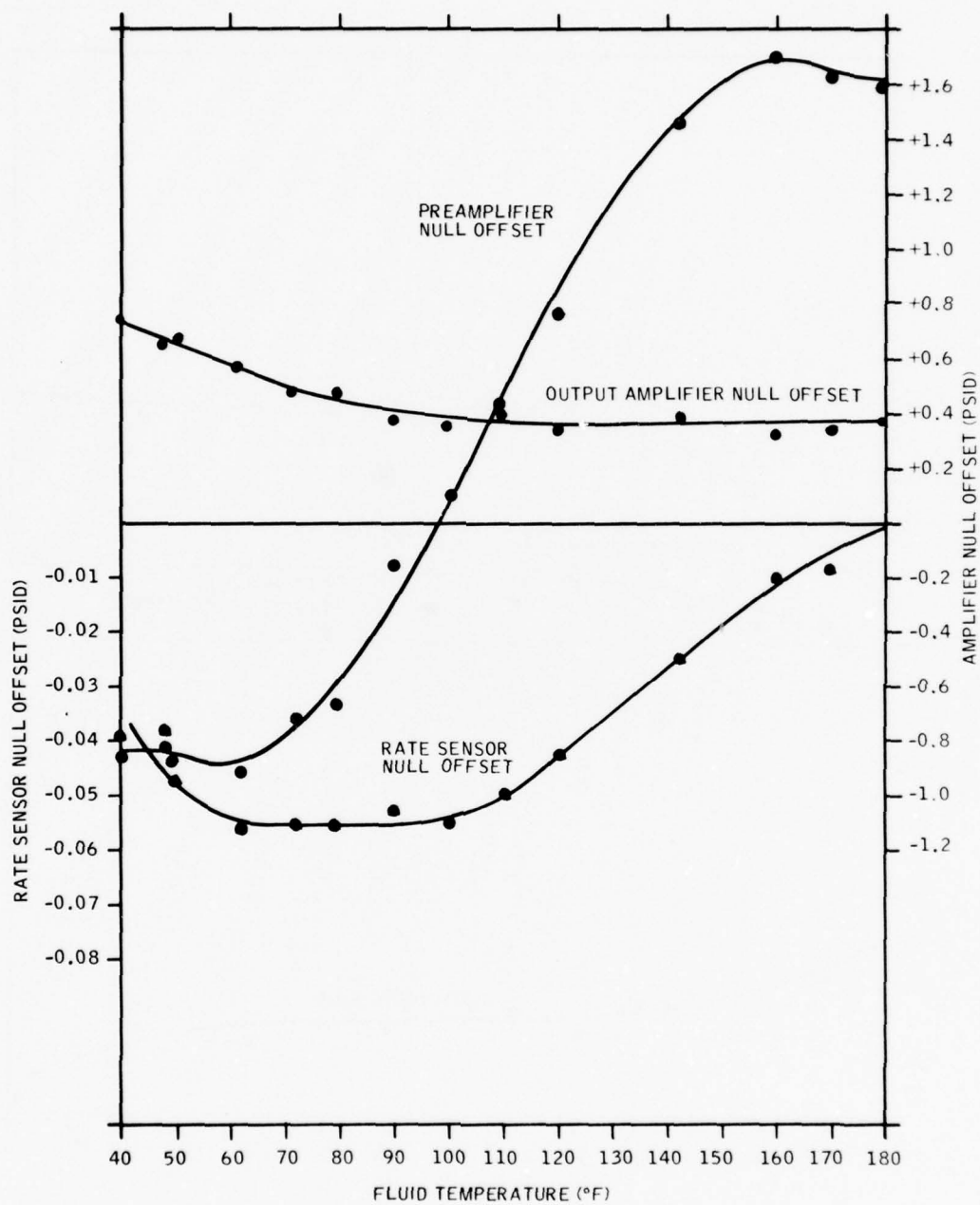


Figure 33. Configuration One Null Offset Characteristics.

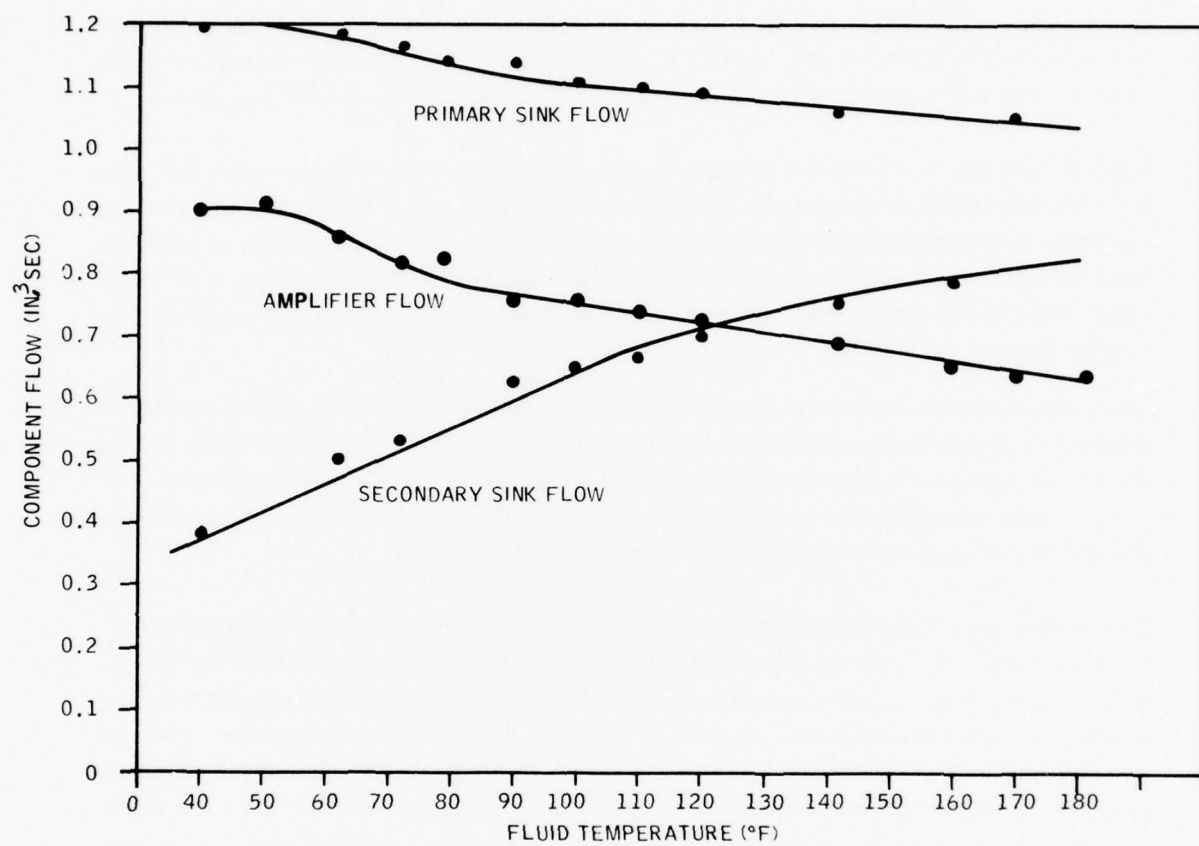


Figure 34. Configuration One Flow Split Characteristics.

Effects of control pressure were discussed in Section III, and typical curves were shown in Figures 17 and 18. Additional parametric data on Configuration one was taken to better define the effects of back pressure (control pressure level) on system gain. The data is presented in Figure 35. Note that the normal operating control pressure level is the highest P_c shown on these curves. It can be seen that a reduction in control pressure level will improve low temperature gain while reducing the high temperature gain to about 0.1 psid/deg/sec. A viscosity sensitive restrictor in the amplifier return line would reduce P_c more at cold temperature than at high temperature.

Configuration two incorporated a viscosity sensitive restrictor in the rate sensor return line. This restrictor assembly is shown partially disassembled on the right side of Figure 10. System gain as a function of temperature with this back pressure restrictor improved substantially at cold temperature; however, the gain dropped off sharply at high temperature as shown in Figure 36. It was observed during this testing that a decrease in amplifier flow at high temperature would result in a higher gain.

Configuration three is the same as two with a 4-percent reduction in amplifier flow. Gain characteristics of this configuration are shown in Figure 37. High temperature gain is excellent, but the low temperature gain is degraded by the reduction in amplifier flow. More compensation is required to reduce amplifier flow at high temperature. Increasing the viscosity sensitive resistance of the rate sensor branch should accomplish this improvement.

The number of coupling elements in the rate sensor was reduced from 6 to 4 in Configuration four. It was also necessary to adjust R_{12} so that it would have the proper flow split at 120°F. The amplifier viscosity sensitive back pressure restrictor was also removed for these tests. Gain characteristics of Configuration four are presented in Figure 38. The desired low temperature gain was attained, and only the 180°F point was outside of the ± 20 -percent band objective. Component gains, Figure 39, indicate that the combined gain of the output amplifier and capacitor is nearly constant. The preamplifier has a low temperature gain that is slightly higher than its high temperature gain.

Configuration four's preamplifier null offset (Figure 40) indicates that the high offset at 180 degrees was probably the major cause of the gain decrease.

Flow split as a function of temperature, as shown in Figure 41, was improved slightly as a result of removing two rate sensor coupling element discs. Gain data indicated that further improvements in flow split are not required.

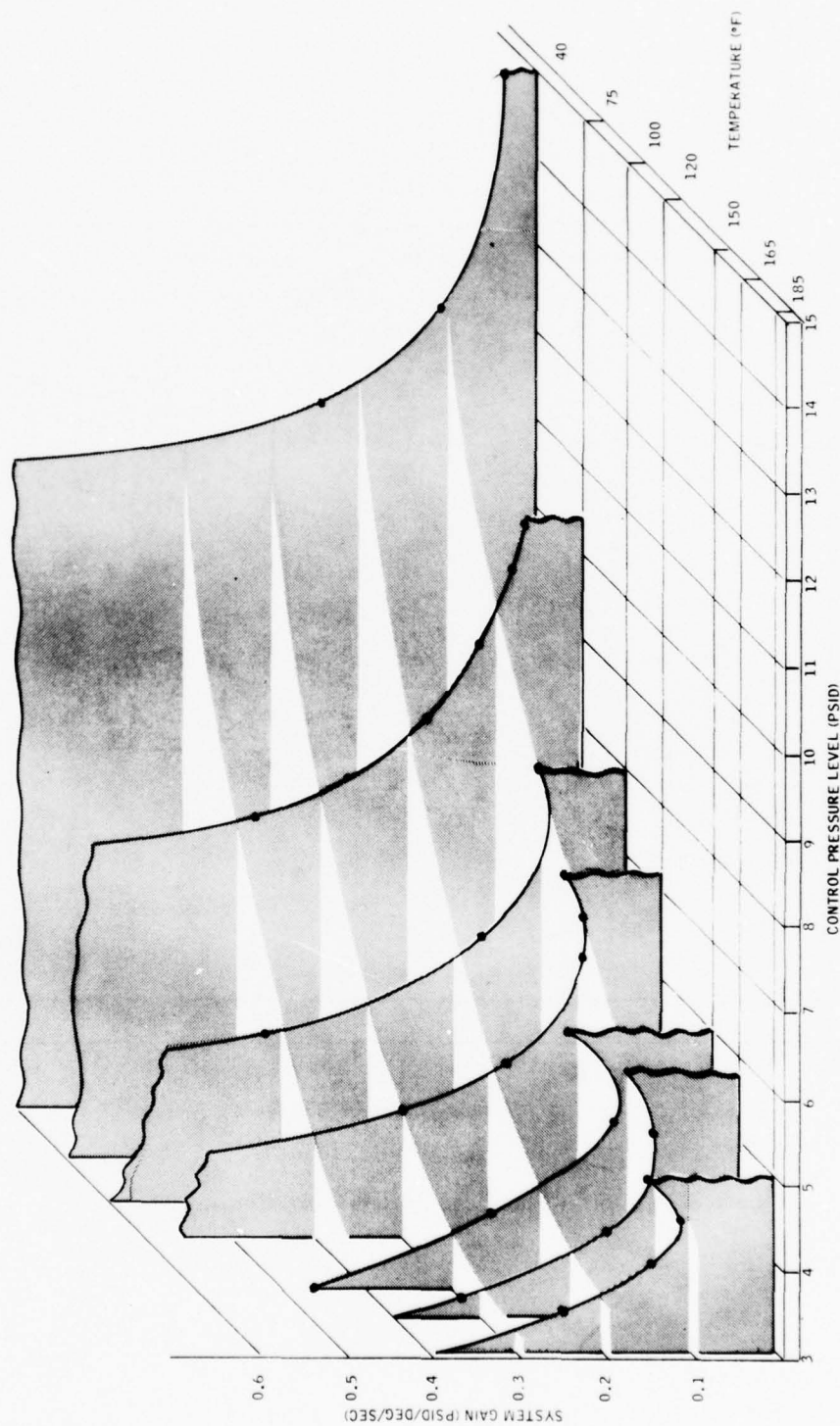


Figure 35. Effects of Control Pressure Level on System Gain.

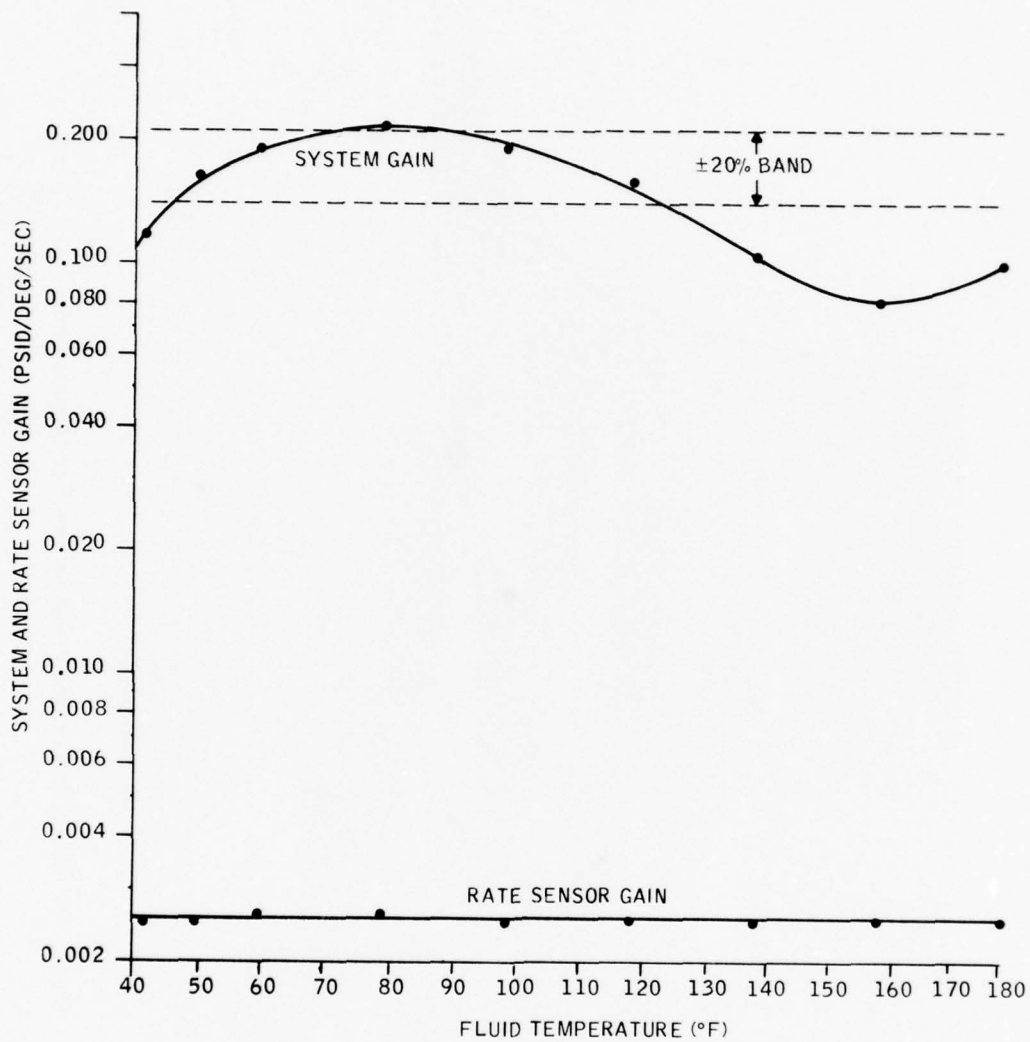


Figure 36. Configuration Two System Gain Characteristics.

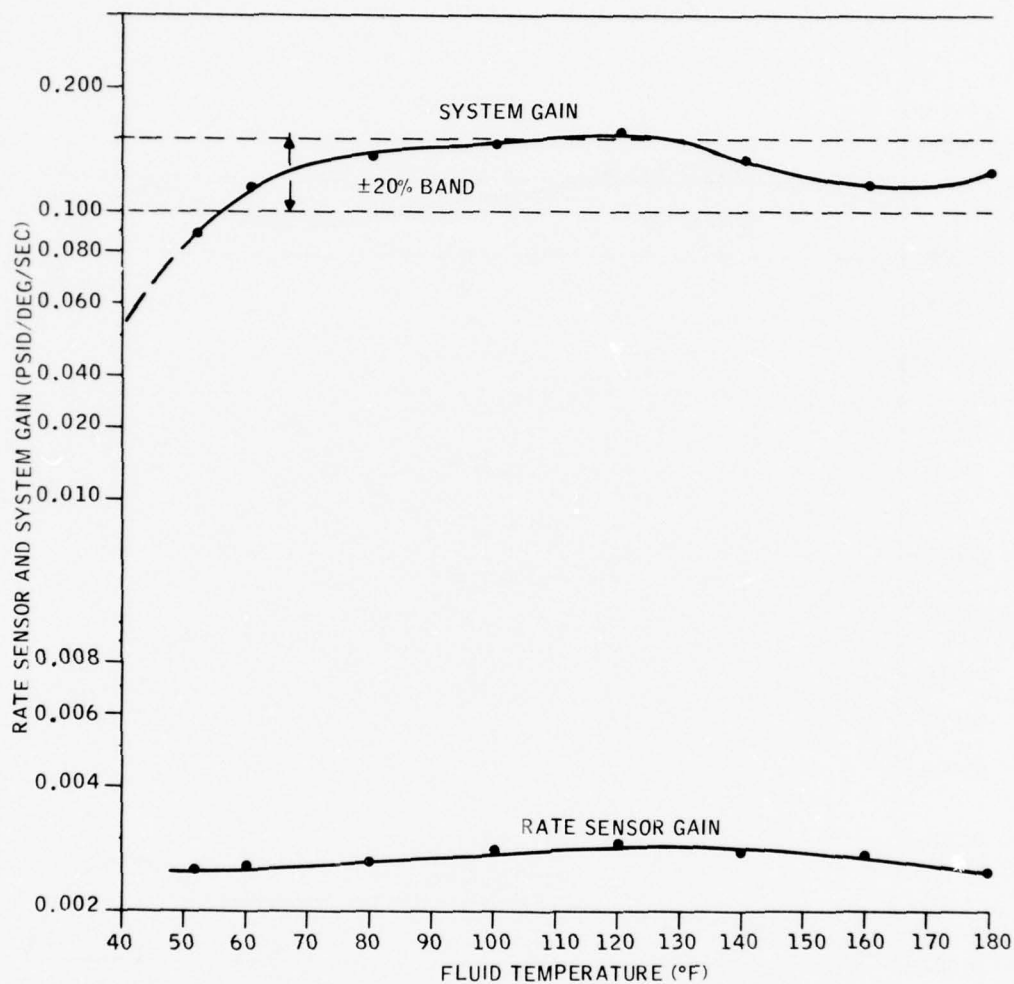


Figure 37. Configuration Three System Gain Characteristics.

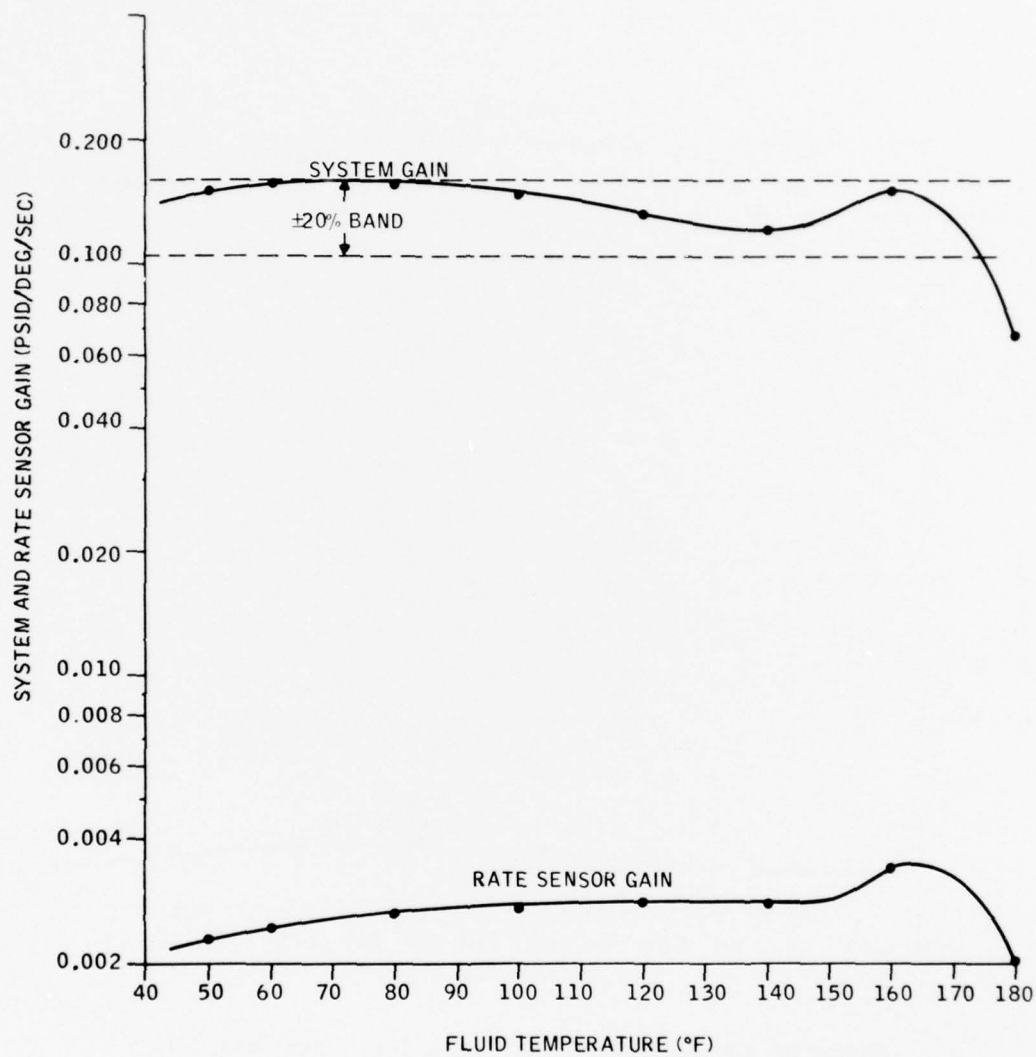


Figure 38. Configuration Four System Gain Characteristics.

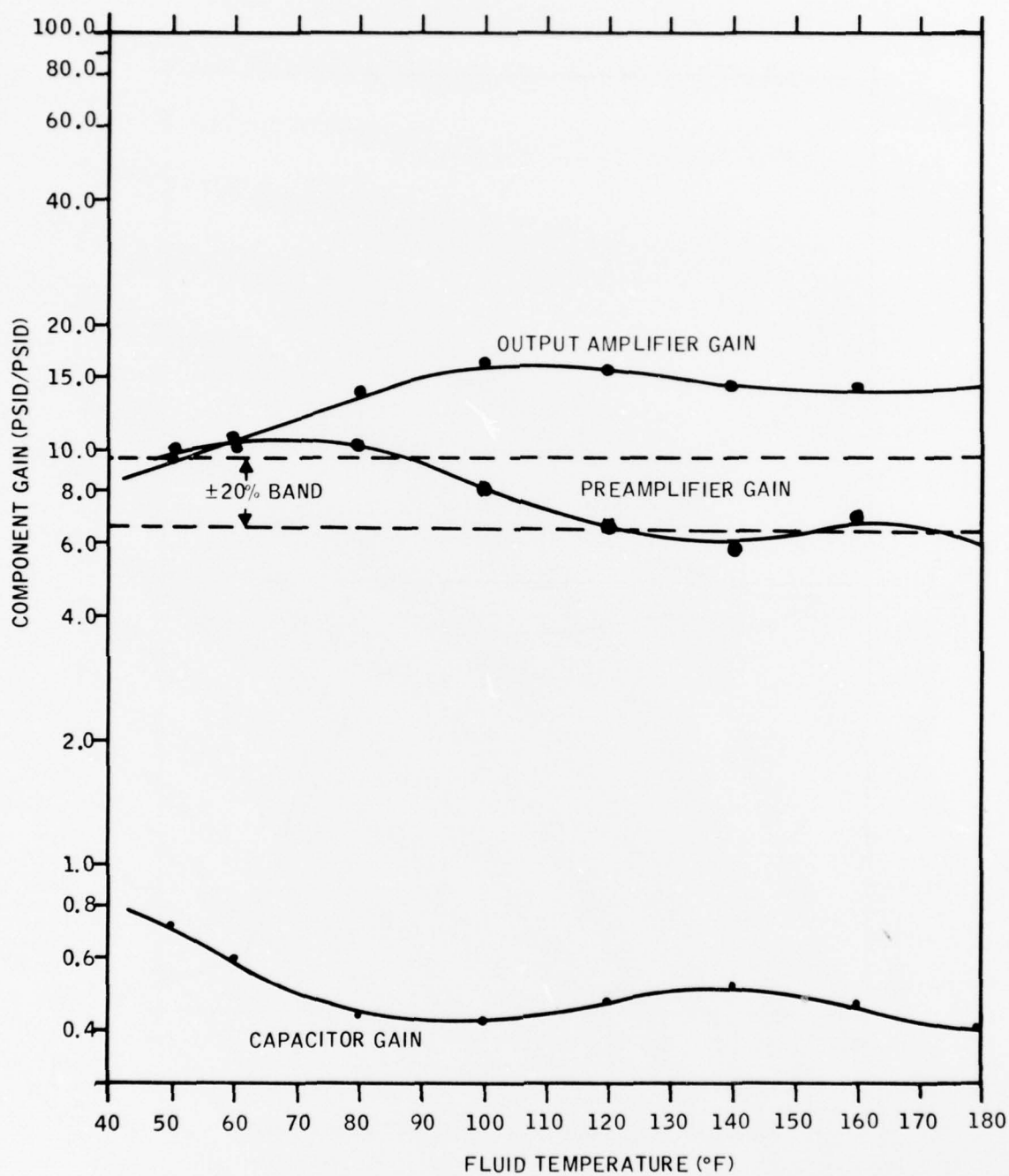


Figure 39. Configuration Four Component Gain Characteristics.

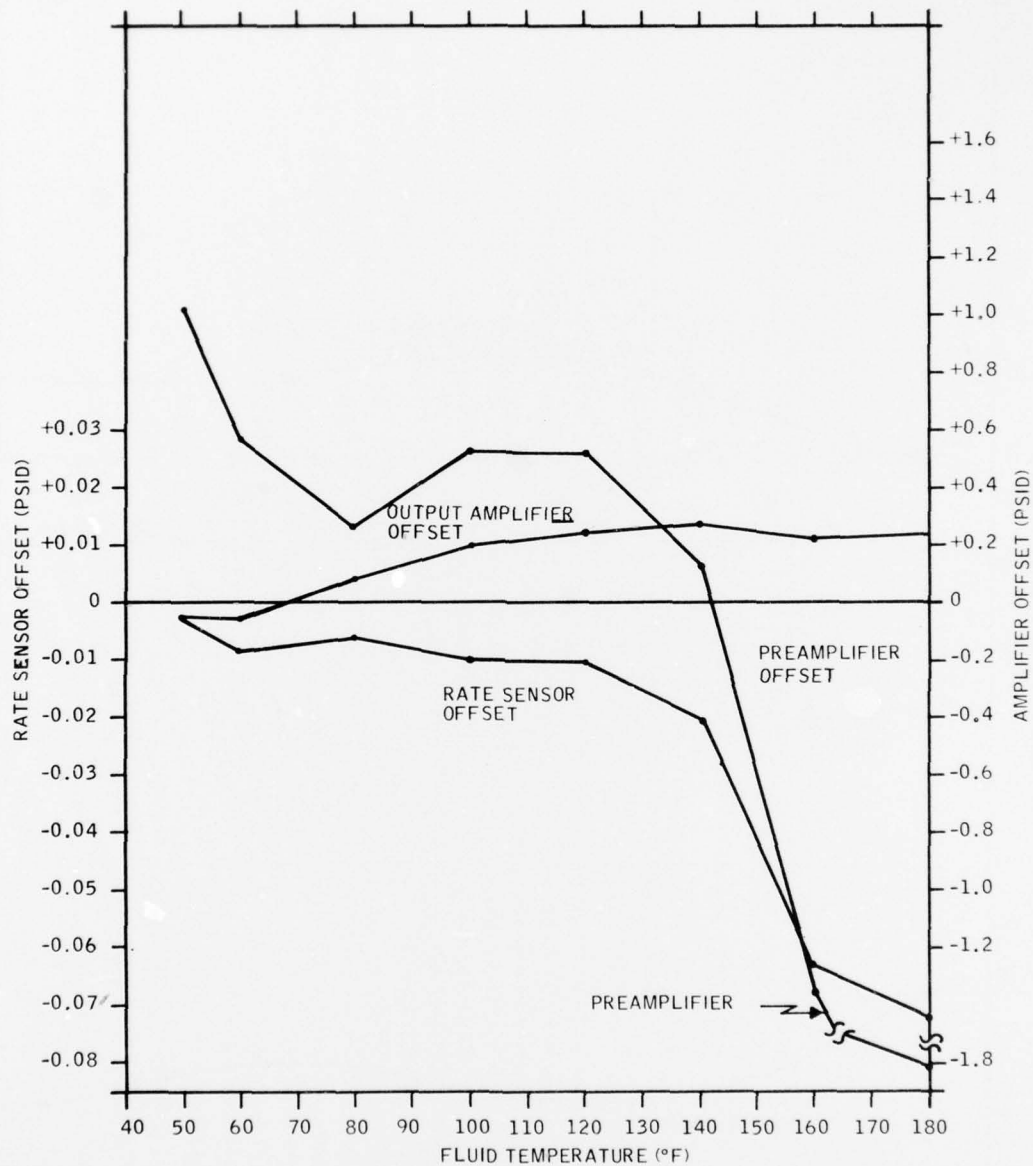


Figure 40. Configuration Four Null Characteristics.

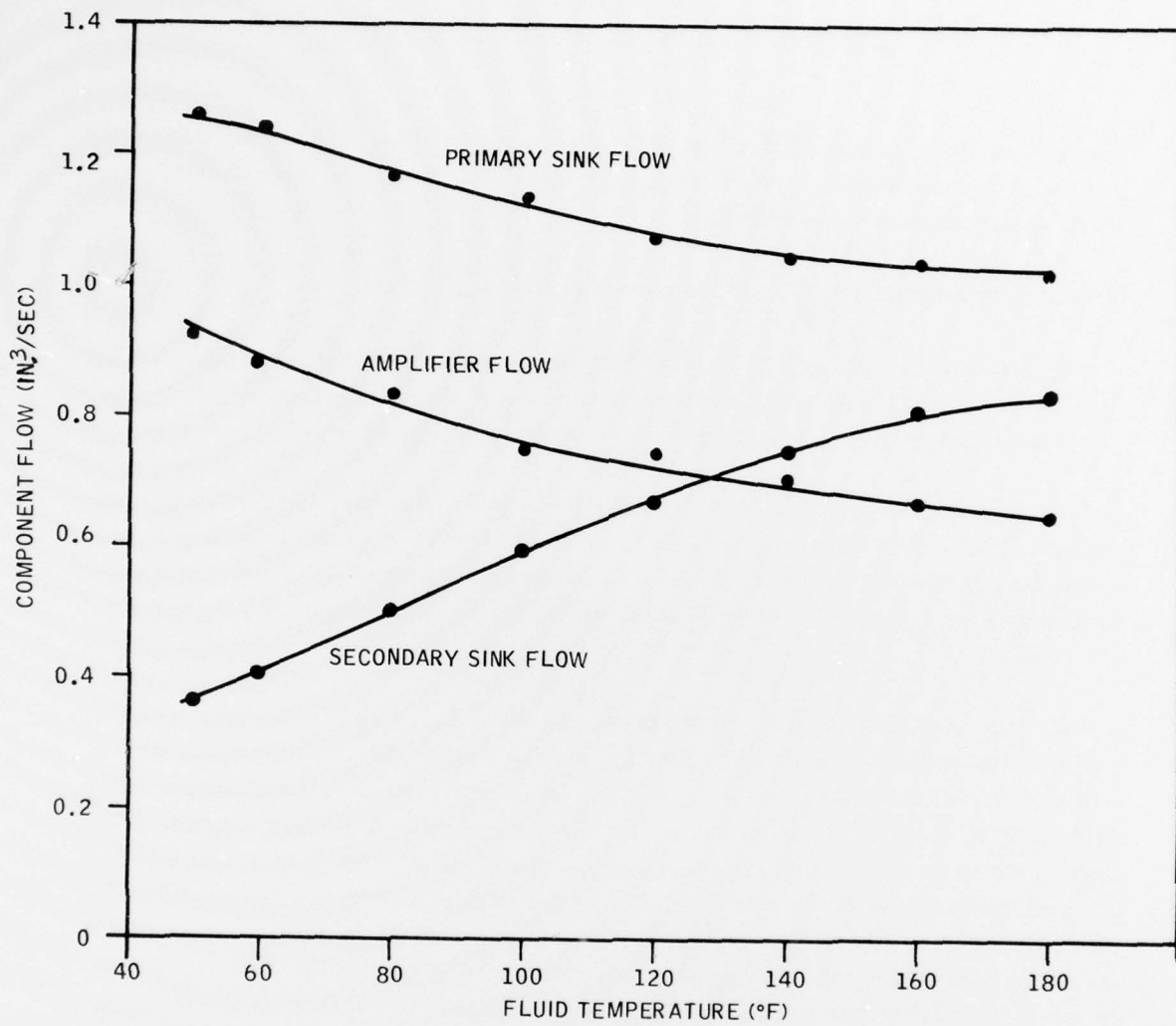


Figure 41. Configuration Four Flow Split Characteristics.

SECTION VII

TESTING OF THE FINAL CONFIGURATION

The final configuration is essentially that of Configuration four. Changes in preamplifier nulling and modifications in amplifier supply resistor R_{12} , introduced during final configuration testing, altered system characteristics slightly.

Investigations conducted on the final configuration were directed to:

- Determining the optimum preamplifier bias resistor configuration for minimum null offset
- Determining the cause of unusual performance at 180°F fluid temperature
- Determining system gain sensitivity to both flow and temperature

Maintaining a constant gain over the 40° to 180°F temperature range requires a reasonably stable preamplifier null offset. Excessive preamplifier null offset, which occurs at some temperatures, results in a decrease in system gain. Several previous temperature tests had to be aborted because the null offset was excessive; a new null offset was adjusted into the system, and the entire test was rerun.

A study was undertaken to improve preamplifier null offset. An x-y plotter was used to generate curves of preamplifier null offset as a function of amplifier supply pressure and as a function of control pressure level (mass ratio). In a systematic sequence of tests in which the bias resistors were varied at 100°F, a dramatic reduction in null offset sensitivity to changes in both amplifier supply pressure and control pressure level was accomplished. A summary of the preamplifier bias configurations investigated and a qualitative evaluation of their performance is presented in Figure 42. Later testing showed, however, that this bias resistor configuration change had no effect in improving preamplifier null offset as a function of temperature (Table 6). Note that with the exception of the 140°F data, preamplifier null offset at each temperature is insensitive to changes in system flow.

Unusual system performance was often observed at 180°F: gain sometimes increased, as shown in Figure 11, and sometimes decreased, as shown in Figure 38. Additional tests were conducted at 180°F to define precisely system characteristics at 180°F. Amplifier flow and pressure are primarily determined by orifice R_{12} ; however, pressure can be reduced further by closing off a variable valve in the modified controller housing (Figure 10). Because the variable valve is sensitive

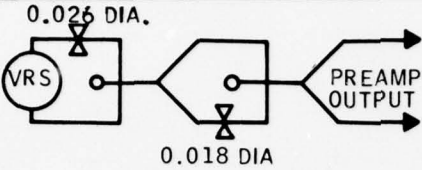
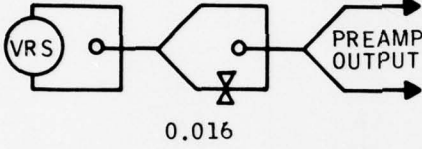
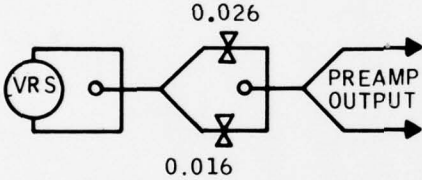
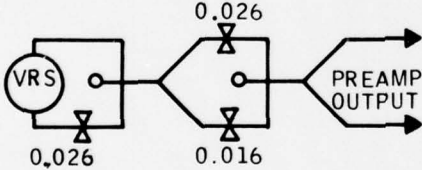
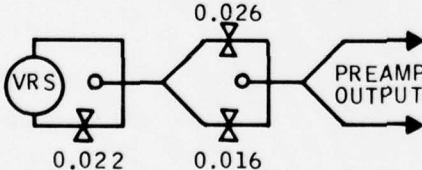
BIAS CONFIGURATION	NULL TOLERANCE TO SUPPLY PRESSURE VARIATIONS	NULL TOLERANCE TO CONTROL PRESSURE LEVEL VARIATIONS
	VERY POOR	VERY POOR
	FAIR	VERY POOR
	POOR	POOR
	GOOD	FAIR
	VERY GOOD	GOOD

Figure 42. Preamplifier Null Offset Study Summary.

TABLE 6. YG1143 FLOW SENSITIVITY TEST DATA

Fluid Temperature (°F)	Fluid Flow in. ³ /sec	Nominal Flow Point	System Gain (psid/deg/sec)	System Null Offset (psid)	Preamplifier Null Offset (psid)
40	2.341	Nominal	0.031	-0.10	-2.88
40	2.450		0.035	-0.12	-2.93
40	2.560		0.043	-0.14	-3.05
40	2.674		0.053	-0.15	-3.09
40	2.786		0.063	-0.15	-3.14
60	2.282	Nominal	0.082	-0.20	-1.23
60	2.402		0.094	-0.32	-1.23
60	2.464		0.096	-0.23	-1.27
60	2.513		0.102	-0.21	-1.27
60	2.564		0.105	-0.22	-1.30
60	2.626		0.108	-0.21	-1.30
60	2.743		0.115	-0.20	-1.33
80	2.299	Nominal	0.100	-0.10	-1.00
80	2.410		0.109	-0.10	-1.04
80	2.480		0.112	-0.10	-1.08
80	2.529		0.113	-0.12	-1.10
80	2.580		0.115	-0.10	-1.13
80	2.649		0.119	-0.08	-1.15
80	2.761		0.124	-0.05	-1.18
100	2.249	Nominal	0.107	-0.04	-0.66
100	2.359		0.116	-0.01	-0.67
100	2.428		0.123	-0.00	-0.68
100	2.478		0.103	-0.01	-0.67
100	2.528		0.136	-0.00	-0.65
100	2.599		0.143	+0.01	-0.62
100	2.710		0.158	+0.05	-0.45
140	2.240	Nominal	0.128	+0.20	+0.94
140	2.360		0.111	+0.22	+1.50
140	2.430		0.094	+0.27	+1.93
140	2.480		0.087	+0.28	+2.10
140	2.530		0.085	+0.29	+2.29
140	2.599		0.066	+0.33	+2.58
140	2.719		0.040	+0.35	+3.09
175	2.262	Nominal	0.104	+0.30	+1.08
175	2.381		0.116	+0.35	+1.13
175	2.499		0.118	+0.42	+1.20
175	2.619		0.137	+0.40	+1.07
175	2.739		0.120	+0.40	+1.05

to viscosity, a smaller R_{12} was used and the variable valve was opened completely to eliminate its viscosity sensitive resistance. The sequence of testing and results are summarized in Table 7. Initial testing at 180°F showed that system gain reached 0.12 psid/deg/sec when the amplifier supply was 12 psid, and it decreased at lower pressure (gain reduced to 0.1 psid/deg/sec at 10 psid). In Test Condition No. 2, the supply orifice was reduced to 0.030 inch in diameter and the amplifier supply pressure was reduced somewhat more than desired to a level of 10.3 psid. Gain was expected to be about 0.08 psid/deg/sec under these conditions, but it was 0.14 psid/deg/sec. At Test Condition No. two, the gain remained high even when the amplifier supply pressure was reduced to 7 psid.

It was assumed that amplifier gain would be the same at a given supply pressure regardless of the type of restrictor used to obtain the pressure. However, because of the system's unusual performance, it was suspected that some change had occurred when the upper manifold was removed to change R_{12} . Condition No. 3 was a repeat of Condition No. 1 to determine if the change was repeatable. Performance at Condition No. 3 was identical to Condition No. 1. Results of the complete series of tests (Table 7) strongly suggest that the shape or characteristic of the

TABLE 7. POWER SUPPLY TESTS AT 180°F

Test Condition	Preamplifier Supply Pressure (psid)	Nominal Gain at 180°F (psid/deg/sec)	Comments
No. 1 $R_{12} = 0.032$	12.5 Valve open, 11 as tested.	0.10 as tested (0.12 psid/deg/sec at 12 psid)	Gain at 180°F was low, and decreased sharply as amplifier was reduced.
No. 2 $R_{12} = 0.030$	10.3 Valve open (as tested)	0.14	Gain improved at 180°F, and gain versus preamplifier supply pressure was constant. There is slight curvature in the output gain curve.
No. 3 $R_{12} = 0.032$	Same as 1	Same as 1	Same as Test Condition No. 1 performance.
No. 4 $R_{12} = 0.031$	10.5	0.115	Good performance similar to Test Condition No. 2 except Gain is slightly lower. Gain versus preamplifier supply pressure was very good.
No. 5 $R_{12} = 0.029$	10.0	0.09	Similar characteristics as Test Condition No. 1 but somewhat better.

amplifier cascade power supply restrictor is significant in determining cascade characteristics, even if the supply pressure remains unchanged.

Changes in null and gain due to the power supply distribution system were never considered serious in previous development programs and, therefore, were not thoroughly investigated. The prevailing theory is that power supply flow disturbances (double cell swirl combined with single cell swirl) are the cause of both null offset and gain change. Flow straighteners at the power nozzle inlet should correct this problem. Development is required to design an effective flow straightener with minimum pressure drop, small size, and low cost. A long power nozzle such as used on the I.D. amplifiers may be satisfactory under most conditions. Effects of power supply disturbances (swirl) are most noticeable at high temperature, when the oil viscosity is too low to damp out these disturbances.

Investigation of swirl was beyond the scope of this program but should be emphasized in future development programs. Other problems such as temperature compensation, impedance matching, noise, linearity, and response have been greatly diminished.

The objectives of the final series of tests on this program were to determine system sensitivity to flow over the entire temperature range and to define requirements for an uncompensated flow regulator for this system.

Characteristics of the final configuration of the modified YG1143 controller are summarized below.

- Standard amplifiers used throughout.
- Rate sensor supply resistor, R_1 , drilled out.
- Number of primary coupling elements reduced from 34 to 4. Spacers used to maintain proper plate spacing.
- Secondary sink sharp-edged orifice, R_2 , removed and replaced with a viscosity sensitive resistor consisting of four parallel elements in series with five parallel elements.
- Amplifier power supply valve opened completely.
- An amplifier power supply resistor, R_{12} , of 0.030 inch in diameter was used.

- A preamplifier bias of the configuration shown in Figure 43.
- Flow control valve removed.

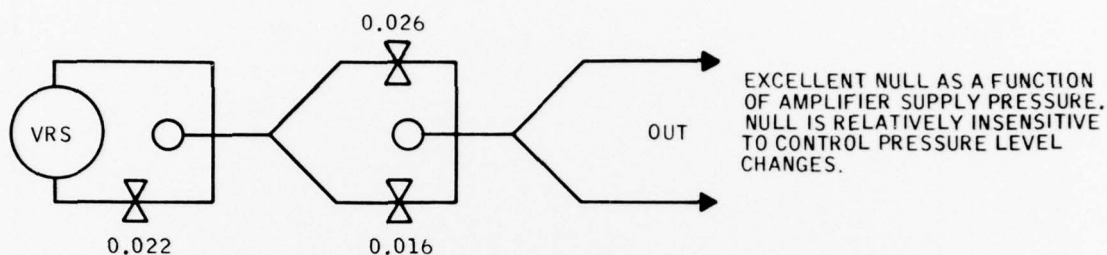


Figure 43. Preamplifier Bias of the Final Configuration.

With the system flow control valve removed, total system flow was varied using an external valve. Tests were performed over the temperature range 40° to 175°F, and flow was varied approximately ± 10 percent about the nominal flow that had previously occurred with the system flow regulator installed. Test data is presented in Table 6.

Gain as a function of temperature for the nominal flow is shown in Figure 44. Gain is within the ± 20 -percent band over the temperature range 50° to 180°F, which is very close to the program objective of ± 20 percent over the temperature range 40° to 180°F.

System gain as a function of total flow is plotted in Figure 45 for all six temperature conditions. A system gain change of 5 percent per percent flow change at 40°F is less than anticipated, and it improves to about 2 percent per percent flow at the higher temperatures. Both theory and experience indicate that system gain should increase with increasing flow. Gain characteristics at the 140°F condition are an exception; the cause was a large variable null offset. This 3-psid null offset, given in Table 6, is nearly equal to the preamplifier output range at 140°F. (The 3-psid null offset at 40°F is much less serious, as the amplifier output range is several times as high at the cold temperature condition.) Because the 140°F negative temperature characteristic is not representative of normal fluidic system performance, these data were not used in establishing the flow regulator requirement.

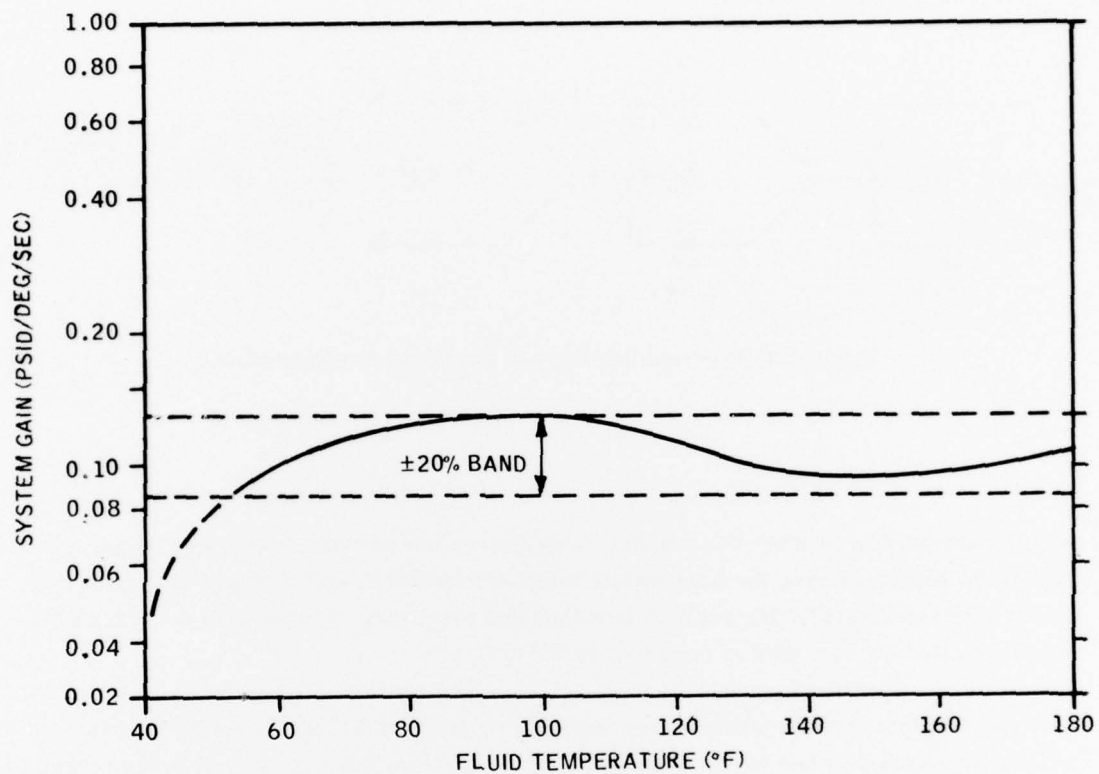


Figure 44. System Gain as a Function of Temperature - Final Configuration.

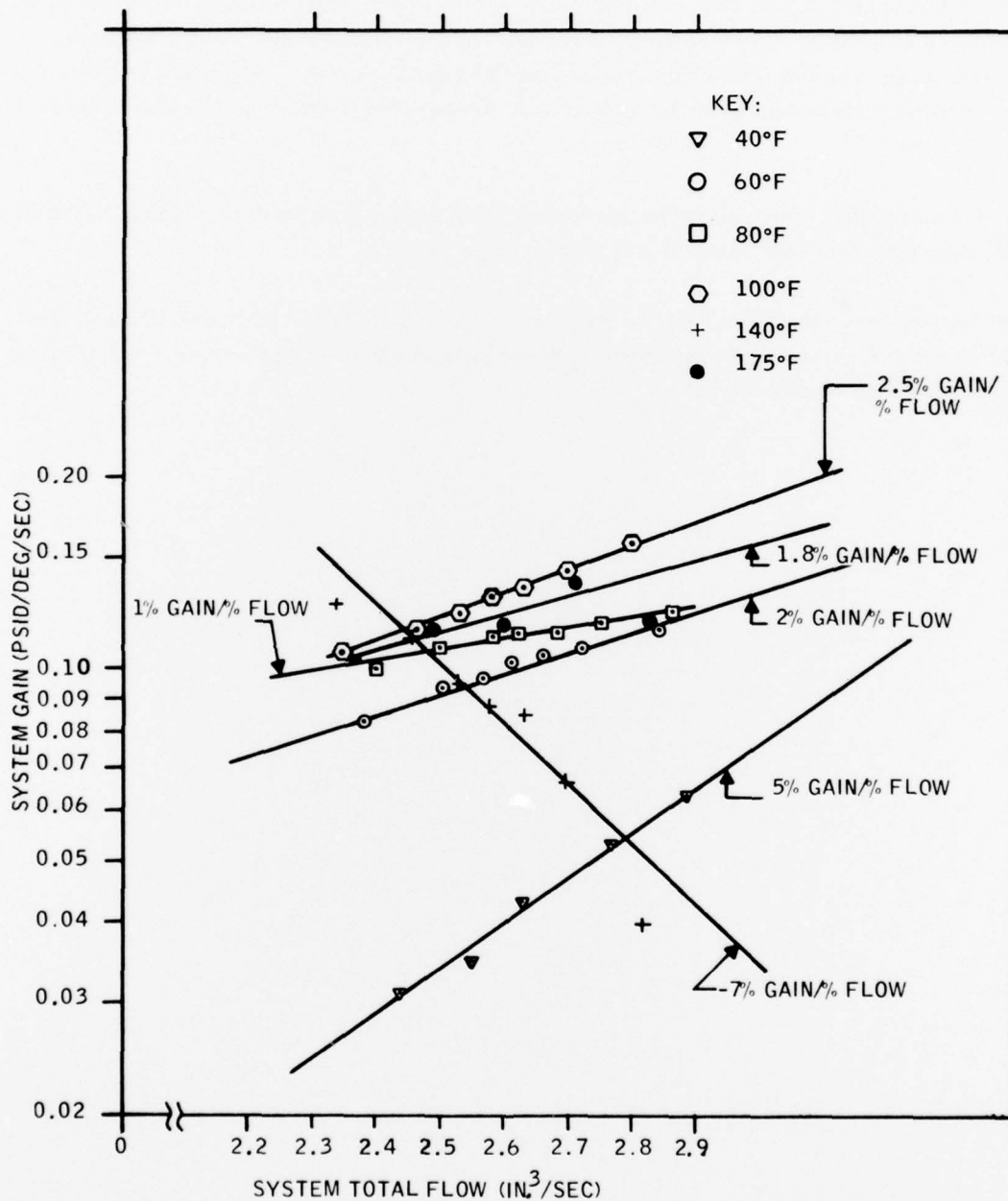


Figure 45. System Gain as a Function of Total System Flow — Final Configuration.

The flow regulator requirement was established to be ± 1 percent, the same as recommended in Reference 2. Addition of temperature compensation did not substantially increase system sensitivity to changes in flow. The uncompensated regulator used in this system is small, low cost, and very reliable when compared with regulators that are required to schedule flow as a function of temperature.

System output null, recorded during this final series of tests, is also included in Table 6. Output null remained within the range of ± 20 percent (± 0.4 psid).

Output noise was always less than the ± 0.2 -psid limit for the YG1143 controller. Compensation techniques used on this program tended to reduce high-temperature noise, and low-temperature noise was almost undetectable.

SECTION VIII CONCLUSIONS

This program established techniques for designing the proper impedance characteristic into each flow path of a system to provide gain compensation over the fluid temperature range of 40° to 180°F without the use of additional compensation networks. Gain of the compensated system is relatively insensitive to flow changes, making it practical to use a simple, low-cost, standard flow regulator. Compensation was accomplished with an insignificant increase in the number and complexity of system parts. Cost and reliability of the compensated hardware should be essentially the same as that for uncompensated hardware.

DEPARTMENT OF THE ARMY

Applied Technology Laboratory
U.S. Army Research and Technology
Laboratories (AVRADCOM)
DAVDL-EU-TSD
Fort Eustis, Virginia 23604

OFFICIAL BUSINESS

PENALTY FOR PRIVATE USE, \$300

POSTAGE AND FEES PAID
DEPARTMENT OF THE ARMY
DOD-314



THIRD CLASS